Sveriges lantbruksuniversitet
Swedish University of Agricultural Sciences

Department of Soil and Environment

Solubility of arsenic in Swedish contaminated soils
– experiments and modelling

Ann-Sophie Heldele

Master's Thesis in Environmental Science
EnvEuro – European Master in Environmental Science

Examensarbeten, Institutionen för mark och miljö, SLU
2016:21

Uppsala 2016

Solubility of arsenic in Swedish contaminated soils – experiments and modelling

Ann-Sophie Heldele

Supervisor: Jon Petter Gustafsson, Department of Soil and Environment, SLU
Assistant supervisor: Thilo Rennert, University of Hohenheim
Examiner: Dan Berggren Kleja, Department of Soil and Environment, SLU

Credits: 30 ECTS
Level: Second cycle, A2E
Course title: Independent Project in Environmental Science - Master´s thesis
Course code: EX0431
Programme/Education: EnvEuro – European Master in Environmental Science 120 credits

Place of publication: Uppsala
Year of publication: 2016
Title of series: Examensarbeten, Institutionen för mark och miljö, SLU
Number of part of series: 2016:21
Online publication: http://stud.epsilon.slu.se

Keywords: arsenic, leaching, pH influence, geochemical modelling, contamination

Sveriges lantbruksuniversitet
Swedish University of Agricultural Sciences

Faculty of Natural Resources and Agricultural Sciences
Department of Soil and Environment

Abstract

Even though arsenic can be found everywhere in the environment, it is phytotoxic and hazardous to human and animal health. Especially arsenic leaching produces contamination of groundwater. But a number of factors, such as the amount and type of adsorbing soil constituents, pH value, redox conditions and residence time have an important influence on the potential mobility and leachability of arsenic. Especially the presence of hydrated oxides and hydroxides of Fe, Al and Mn have an essential influence.

In this study two heavily contaminated Swedish soils have been investigated on the arsenic solubility as a function of pH with the aid of batch experiments. The sites were a former wood impregnation site (Åsbro) and an area of a former glass factory (Pukeberg). The results of the batch experiments were evaluated using geochemical modelling (Visual MINTEQ). The objective of the study was to assess if a change in the soil pH could lead to an increased leaching of arsenic from the two contaminated soils. Furthermore, the plausibility of geochemical modelling as a tool in risk assessment was explored. The hypothesis of a low arsenic leachability for pH above 3 and that arsenic is mainly adsorbed to ferric (hydr)oxides were stated.

The study showed that at least in one of the soils, ferric (hydr)oxides were not the main phase controlling As solubility. For the other soil no explicit statement on the role of ferric (hydr)oxides as adsorption sites for arsenic could be made. Furthermore, the assumption that arsenic adsorption results in a low leachability of As at pH > 3 was proved to be wrong. The depiction of the experimental results using geochemical modelling proved to be difficult. These results indicate that additional investigations need to be made concerning the reactive solid phases relevant for As in heavily contaminated soils before geochemical models can be used in risk assessment.

Popular Science Summary

Arsenic can be found everywhere in the environment. There are a few natural sources, but the main sources are anthropogenic, e.g. arsenic as a component of pesticides, used in wood preservation, in the manufacturing of glass and through the burning of fossil fuels. The problem is arsenic can have a toxic effect on plant growth and is dangerous to human and animal health. Arsenic can cause acute and chronic poisoning and is especially dangerous in case of long-term exposure through food or air. One of the biggest problems is the leaching of arsenic from soils into the ground water. The fact that the total arsenic concentration does not indicate its potential mobility and leachability makes risk assessments of arsenic-contaminated sites difficult. Other factors such as the amount and type of adsorbing soil constituents, pH value and residence time have to be taken into account.

In soils and waters, arsenic is usually found in its anionic form: as arsenite (AsO_3^{3-}) or arsenate (AsO_4^{3-}). Due to the fact that Fe and Al (hydr)oxides may have a net positive charge below pH 7, and that the soil pH in most natural soils doesn't exceed this value, they are expected to be the main adsorbent minerals for arsenic.

The aim of this study was to assess if a change in the soil pH could lead to an increased leaching of arsenic from two heavy contaminated Swedish soils. This has been examined with the help of batch experiments. The experimental results have been evaluated also with the help of geochemical modelling. A purpose of using geochemical modelling was to explore the plausibility of this tool in risk assessment.

The results showed for both investigated sites that a reduction in the soil pH could lead to an increased leaching of arsenic from the studied contaminated sites. Furthermore it was proven that in at least one of the soils, Fe and Al (hydr)oxides were not controlling the solubility of arsenic. The depiction of the experimental results using geochemical modelling proved to be difficult. These results indicate that more needs to be known about the chemical reactions of arsenic in heavily contaminated soils before geochemical models can be used in risk assessment.

I. Table of contents

II. List of Figures

III. List of Tables

1 Introduction

Arsenic can be found everywhere in the environment, and there are two well-known general sources: on the one hand the natural occurrence of arsenic, for example from volcanism and weathering of bedrock. Secondly there is an anthropogenic source of arsenic, where arsenic is introduced into the environment as a component of pesticides, in wood preservation, in the manufacturing of glass, through the burning of fossil fuels and by smelting of arsenic-bearing minerals (Bisone et al. 2016; Bissen and Frimmel 2003). But why is risk assessment in the context of arsenic so important?

One important reason is the fact that arsenic is phytotoxic as well as hazardous to human and animal health. Therefore, its leaching presents risks to the groundwater quality (Sadiq 1995; Violante and Pigna 2002). Its toxicity, however, depends on its speciation: inorganic arsenic compounds are more toxic than organic arsenic compounds (Bissen and Frimmel 2003).

Moreover, in contrast to organic contaminates, arsenic can be neither decomposed chemically nor biologically (Bisone et al. 2016).

One problem in the risk assessment of arsenic is the fact that the total concentration does not indicate its potential mobility and leachability (Bisone et al. 2016). A lot of factors such as the amount and type of adsorbing soil constituents, the pH value, redox conditions and biological transformations have an important influence on the mobility of arsenic (Bisone et al. 2016; Bissen and Frimmel 2003). The presence of hydrated oxides and hydroxides of Fe, Mn and Al, compounds of Ca, natural organic matter, clay minerals and competing anions (e.g PO_4^{3-}) have an essential influence (Bisone et al. 2016; Dousova et al. 2016). Therefore, to apply suitable management strategies, it is of great importance to recognize the chemical interactions between soil and arsenic (Bissen and Frimmel 2003).

In nature, arsenic can be found in different oxidation states: arsenic (0), arsenate (+V), arsenite (+III) and arsine (-III) (Bissen and Frimmel 2003). Nevertheless, in soils and aqueous environments the most common forms are arsenite and arsenate, although As (III) is usually the dominant form in reduced conditions, while As (V) is more dominant in aerobic environments (Bissen and Frimmel 2003; Sadiq 1995). Arsenic (III) and arsenic (V) demonstrate a high affinity for oxygen. Consequently, in the soil, it is mainly found in oxyanionic forms such as AsO_3^{3-} (arsenite) and AsO_4^{3-} (arsenate) (Sadiq 1995; Bissen and Frimmel 2003). However, while arsenate dissociates in a pH range from 2 to 11 (from H_3AsO_4 to $H_2AsO_4^-$ or $HAsO_4^{2-}$), arsenite appears in the form of H_3AsO_3 till pH 9 and only dissociate to its anion forms for higher pH values (Figure 1) (Bissen and Frimmel 2003). The oxyanions of arsenic tend to form strong inner-sphere complexes specially with variable charge soil minerals like Al ,Fe, and Mn

oxides (Violante and Pigna 2002). Three forms of these surface complexes are possible: a monodentate complex, a bidentate-binuclear complex and a bidentate-mononuclear complex (Violante and Pigna 2002). Nonetheless, the predominant complex form is a bidentate-binuclear complex (Moldovan and Hendry 2005).

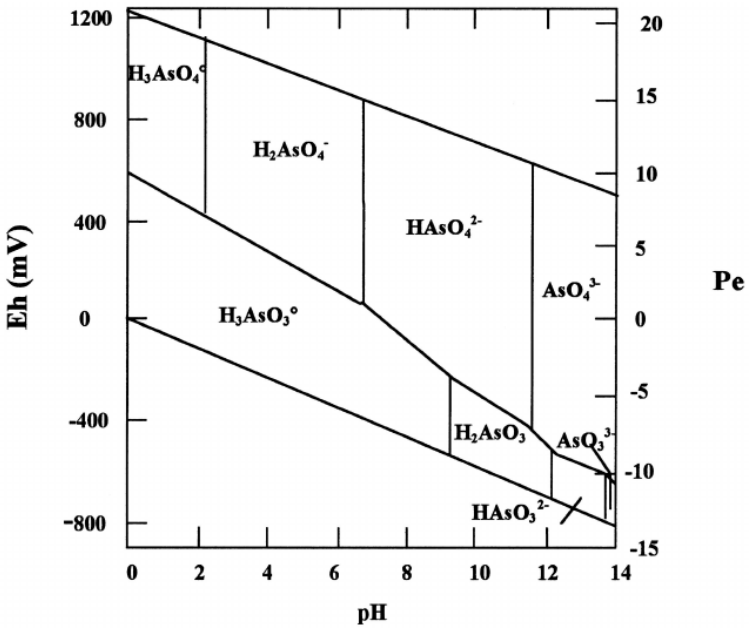

Figure 1 Redox potential (Eh) – pH diagram for aqueous arsenic species in the system AsO_2-H_2O at 25°C and 1 bar total pressure (Adapted from Akter et al. 2005)

For the experiment in my study, two heavy contaminated sites were chosen. The first site is Åsbro, a former wood impregnation site, nowadays owned by Vattenfall AB (Jernlås and Karlgren 2009). Lake Tisaren and several municipalities are located in the vicinity. A study on the site was performed by Vattenfall AB; this included a risk assessment by Kemakta in 2006. The results showed that the amount of arsenic in 50% of the soil profiles exceeded the site-specific threshold of 60 mg/kg As (Jernlås and Karlgren 2009). Samples with amounts as high as 2700 mg/kg As could be found on the area (Jernlås and Karlgren 2009). Also in the sediments of Lake Tisaren, close to the beach, high amounts of arsenic, which may pose a risk to human health, have been found (Jernlås and Karlgren 2009).

The second site is located at Pukeberg, in the area of a former glass factory. Previous risk assessments at this site showed that in large parts of the area, the contamination level exceeds the site-specific guidelines (Elert and Höglund 2012). Especially arsenic and lead were found in such high amounts that they pose a risk for human health (Elert and Höglund 2012). Several residential areas can be found close to the old factory. The nature reserve Svartbäcksmåla borders the area in the South and East (Elert and Höglund 2012). Furthermore, one of south-eastern Sweden's biggest groundwater sources, Nybroåsen, which supplies Nybro city and several other towns with drinking

water, is situated only a few kilometres from the old factory (Elert and Höglund 2012). Also the small river S:t Sigfridsån, which could be used as a drinking water source, flows close to the Pukeberg area (Elert and Höglund 2012).

Therefore, for both sites, leaching of arsenic could have a significant influence on human health, environment and groundwater.

In this study, the solubility of arsenic as a function of pH in the two contaminated soils has been investigated with the aid of batch experiments. Moreover, the results of the batch experiment have been evaluated using geochemical modelling (Visual MINTEQ). The objective was to assess if changes in the soil pH could lead to an increased leaching of arsenic from the two contaminated soils. Furthermore the plausibility of geochemical modelling as tool in risk assessment will be explored. The following hypotheses were stated:

(1) The arsenic present in two contaminated soils is mainly adsorbed to ferric (hydr)oxides
(2) Arsenic adsorption results in a low leachability of arsenic for pH above 3.
(3) It is possible to predict the arsenic solubility in the two studied soils with the help of geochemical modelling.

2 Background

The fate of arsenic in soil is difficult to predict, and therefore a lot of research is going on in behalf of the chemical behaviour of arsenic in soils:

An investigation on the effects of soil properties on arsenate adsorption was made by Jiang et al (2005). For this purpose, the relationship between adsorption capacity and the properties of 16 Chinese soils was modelled, and the resulting model was validated against three Australian and 3 American soils (Jiang et al. 2005). According to the model, citrate-dithionite extractable Fe (Fe_{CD}) had the most important positive influence on arsenic adsorption, whereas DOC was negatively correlated with arsenic adsorption (Jiang et al. 2005). Moreover, SOM suppressed the As adsorption on low-energy adsorption sites, in contrast to the clay content, which had a positive influence (Jiang et al. 2005).

A complete risk assessment, including the examination of historical records, solid-phase characterisation and chemical modelling, was performed by Lumsdon et al. (2001) on an industrially contaminated site. At this site, the principal reactive adsorbent for arsenic was ferric hydroxide. Furthermore, the results from batch equilibrium experiments, which showed an increased mobility of arsenic at increasingly alkaline conditions, could be successfully predicted by a model prepared with the help of the computer programme ECOSAT (Lumsdon et al. 2001). It was concluded that it was necessary to identify the reactive solid phases first and to have an appropriate database containing metal surface complexation constants, before starting a modelling approach on other contaminated sites (Lumsdon et al. 2001).

A similar experiment was conducted by Bisone et al. (2016). Here a highly arsenic-contaminated gold mining site in France was analysed for the mobility and fractionation of arsenic, by combining experimental data (leaching tests), mineralogical characteristics and geochemical modelling. The results of the experiment showed, that on this site, most of the arsenic was reversibly adsorbed onto Fe phases in the soil particles, especially Fe oxyhydroxides (Bisone et al. 2016). In addition, the geochemical modelling supported the experimental results (Bisone et al. 2016). However, the results led to the conclusion that especially under acidic or reducing conditions, which usually can be found in mining environments, a potential risk of As mobilisation is present (Bisone et al. 2016).

All the above mentioned investigations showed the importance of iron hydroxides in influencing the solubility of arsenic. This role of iron minerals was also emphasised by Moldovan and Hendry (2005), who conducted an experiment at the Rabbit Lake uranium mine site (Saskatchewan, Canada) with the objective of determining the controls on the solubility of dissolved arsenic over a pH range of 1 to 11. Their aim was to develop a thermodynamic database for the dominating mineralogical controls on

arsenic in the mill (Moldovan and Hendry 2005). Geochemical modelling was conducted using the chemistry data, and the results showed that in a pH range from 2.3 to 3.1 the formation of scorodite ($FeAsO_4$:H_2O) was the dominant arsenic controlling factor, while at a pH above 3.1 adsorption to 2-line ferrihydrate was the essential process (Moldovan and Hendry 2005). In the pH range from pH 3.1 to pH 11 about 99.8% of the dissolved arsenic is bound by ferrihydrate (Moldovan and Hendry 2005).

Nevertheless, other investigations have shown that iron phases are not the only possible adsorbents for arsenic in soils.

An attempt of relating the geochemical behaviour of arsenic to its chemical speciation and additionally to identify low-solubility poorly-crystalline metal arsenates was made by Gutiérrez-Ruiz et al. (2012) on Mexican soils which were contaminated by a lead smelter. Thermodynamic equilibrium modelling was used to describe the solubility of arsenic in some of the soil samples (Gutiérrez-Ruiz et al. 2012). The results showed that in the majority of the soil samples As(V) adsorption to Fe (hydr)oxides was not the dominant adsorption process, instead chemical extractions and SEM-EDS analyses indicated that the governing process was the formation of low-solubility Pb arsenates (Gutiérrez-Ruiz et al. 2012). Moreover, the presence of unreacted Ca-arsenates was identified in few of the soil samples. The thermodynamic modelling supported the results by predicting the formation of the Pb arsenate minerals duftite and hydroxymimetite (Gutiérrez-Ruiz et al. 2012).

Moreover, Villalobos et al. (2010) showed in their investigations, which were also performed on Mexican soils contaminated with residues from metallurgical processes, an arsenic mobility predominantly controlled by the formation of Pb, mixed Pb-Cu, and Ca arsenate solids. The experimentally obtained dissolved arsenic concentration values were furthermore simulated, using a database updated for all known metal arsenate formation constants (Villalobos et al. 2010). The results showed that precipitation processes were favoured, despite a high average Fe content of 2% (Villalobos et al. 2010).

The occurrence of Mn oxides can also play an important role in the fate of arsenic as shown by the investigations of Deschamps et al (Deschamps et al. 2003). The adsorption capacity of arsenic was investigated by performing a detailed mineralogical identification on samples naturally containing Mn and Fe (Deschamps et al. 2003). It was indicated by the outcome, that the presence of Mn minerals in the sample promoted the oxidation of As(III) to As(V) (Deschamps et al. 2003). Furthermore, the outcome showed that a significant adsorption of both arsenic species by the Mn minerals occurred, even though the adsorption was not as high depicted as by the Fe minerals occurring in the sample (Deschamps et al. 2003).

The solubility of arsenic is additionally influenced by other anions. An example is the influence of phosphate, as shown by Chien et al. (2012) who analysed the adsorption

characteristics of aqueous As(V) and As(III) in Taiwan soils through batch adsorption experiments. The experimental results showed that the adsorption strength of the soils increased with increasing amounts of Fe, Mn and Al oxides, that the adsorption of As(V) was higher than that of As(III), and that the concentration of phosphate in the soil was negatively correlated with the adsorption of aqueous arsenic species (Chien et al. 2012).

The influence of phosphate was also analysed by Smith et al. (2002) who investigated the effect of PO_4^{3-}, Na^+ and Ca^+ on the sorption of the two arsenic species, As(V) and As(III), in different soil types in Australia. Their study showed that the presence of phosphate in solution had a suppressing effect on the sorption of both arsenic species, but the effect varied depending on the sorption capacity of the soil (Smith et al. 2002). In soils containing low amounts of Fe oxides, arsenic adsorption was strongly influenced by PO_4^{3-}, while the same amount of PO_4^{3-} showed only a slight influence on arsenic adsorption in soils with high Fe content (Smith et al. 2002). Moreover, an increase of dissolved P did not result in a decreased adsorption of As(V), suggesting that some oxide surfaces may contain preferential sorption sites for As(V) (Smith et al. 2002).

In addition, Violante and Pigna (2002) investigated the following factors for their influence on the competitive sorption of AsO_4 and PO_4 in soil: pH (4-8), ligand concentration, surface coverage of the oxyanions in the samples and the residence time (Violante and Pigna 2002). The results suggest that the mobility, the bioavailability and the toxicity of arsenic in soil environments is greatly affected by the nature of soil components, pH, initial AsO_4/PO_4 molar ratios and residence time (Violante and Pigna 2002).

The same influence of anions was shown by Xu et al. (1988), who investigated the adsorption of As(V) on alumina, hematite, kaolin and quartz as a function of pH and arsenic concentration. Moreover, the influence of sulphate and fulvic acid on the adsorption of As(V) was examined (Xu et al. 1988). The results of the experiment showed that the most important parameters affecting the adsorption of arsenic were the charge of the solid surface and the As speciation in solution, while the adsorption was reduced by the presence of sulphate and/or fulvic acid (Xu et al. 1988).

The source of arsenic contamination might also have a great influence on the solubility of arsenic. One example is contamination through CCA (cromated copper arsenates), a solution which was used for the preservation of wood (Jang et al. 2002). Because the metal concentrations in the CCA solution are so high, small leakages or spills may cause serious contamination of the soil (Jang et al. 2002). The latter authors investigated the leaching behaviour of arsenic, chromium and copper at a wood preservation site, where CCA had been applied for several years, by performing two common batch leaching tests (Jang et al. 2002). Furthermore, some of the parameters (pH, leaching

time, and liquid/solid ratio), having an effect on the release of these metals, were evaluated. For arsenic, the results indicated metal complexation with acetate ion (Jang et al. 2002). The dissolution of these complexes led to an increase in leachability of arsenic for decreasing pH values (Jang et al. 2002).

CCA-contaminated soil was investigated also by Gräfe et al. (2008), with the purpose of determining if and how the co-contaminated metal cations (Cu, Zn, Cr) influenced the speciation of arsenic. The results showed that arsenic occurred mainly as As(V), and moreover the study suggested copper arsenates to be the main As scavengers (Gräfe et al. 2008). Other precipitates such as scorodite ($FeAsO_4{:}H_2O$), adamite (Zn_2AsO_4OH) and ojuelaite ($ZnFe^{3+}{}_2(AsO_4)_2(OH)_2{:}4H_2O$) were found as well (Gräfe et al. 2008). These results suggest that not only surface adsorption reactions, but also co-contaminating metal cations may significantly influence the chemical speciation of arsenic (Gräfe et al. 2008).

Co-contamination by arsenic in metal-contaminated areas is common, and might be important for the adsorption of arsenic. To examine this effect, a study was implemented by Gräfe et al. (2004), in which the co-sorption of As(V) and Zn on goethite at pH 4 and 7 was investigated as a function of final solution concentration. The results showed that the sorption of As(V) and Zn on goethite increased in co-sorption experiments, compared to single sorption systems. For example at pH 4, arsenate adsorption on goethite increased by 29% in the presence of Zn and by more than 500% at pH 7 (Gräfe et al. 2004). An even stronger increase in the adsorption of Zn on goethite in the presence of As(V) was found, about 800% at pH 4 and 1300% at pH 7 (Gräfe et al. 2004).

3 Materials and Methods

3.1 Soil samples

For the experiment two heavy contaminated sites were chosen:

Åsbro is located in the Örebro County. Since the beginning of the 19th century, an impregnation factory was established on this site, which caused the main part of today's contamination problem, mainly by spilling of the impregnation agent (Jernlås and Karlgren 2009). The impregnation agent used in this area contained (among other things) creosote (PAH) and salts of copper, chromium and arsenic (Jernlås and Karlgren 2009). Arsenic in contents above 60 mg/kg can be found in around 50% of the soil profiles around Åsbro (Jernlås and Karlgren 2009). The highest measured arsenic content is 2700 mg/kg (Jernlås and Karlgren 2009). The soil is sandy with a high content of organic matter (Table 1). Especially As and Cr can be found in relatively high contents (Table 2). For Åsbro 2 layers were examined: the 4-17 cm and the 17-30 cm layers. The soil pH was 6.1 in the top layer and 6.7 in the bottom layer.

Table 1 Compostion of the Åsbro top and bottom layers

Depth (cm)	clay %	silt %	sand %	humus content %
4-17	4.6	20.2	75.3	6.5
17-29	4.7	31.8	63.5	8.1

Table 2 Total contents of As, Fe, Al, Mn, Ba, Cr, Pb and Zn in the Åsbro top and bottom layers

Depth (cm)	As mg/kg	Fe mg/kg	Al mg/kg	Mn mg/kg	Ba mg/kg	Cr mg/kg	Pb mg/kg	Zn mg/kg
0-14	23.40	0.59	1.30	0.48	1.28	0.57	0.07	33.90
14-28	30.15	0.17	0.47	0.14	0.86	1.33	0.03	7.12

The second site chosen for the experiment was **Pukeberg** in south Sweden, where a glass factory was situated. Potash, lime, lead, arsenic, manganese, zinc oxides and nickel oxides for example were used for the glass manufacturing (Elert and Höglund 2012). Several areas around the former glass factory are filled out with residues from the glass production (Elert and Höglund 2012). Probably, the main source of the contamination was through the disposal of manufacturing waste on the backside of the factory, but glass residues were disposed also in the forest surrounding the factory (Elert and Höglund 2012). The natural soil in the area consists of a mix of sand and gravel with a share of stone (Elert and Höglund 2012). The soil from the site investigated in

this experiment is sandy with a small amount of organic matter (Table 3). Metals, such as As, Ba and Pb, were present in high contents in the soils of this site (Table 4). For Pukeberg also two layers were examined: the 0-14 cm and 14-28 cm layers. The pH in both layer was 8.1.

Table 3 Composition of the Pukeberg top and bottom layers

Depth (cm)	clay %	silt %	Sand %	humus content %
0-14	3.7	10.1	86.2	2.3
14-28	3	7	90	1.3

Table 4 Total contents of As, Fe, Al, Mn, Ba, Cr, Pb and Zn in the Pukeberg top and bottom layers.

Depth (cm)	As mg/kg	Fe mg/kg	Al mg/kg	Mn mg/kg	Ba mg/kg	Cr mg/kg	Pb mg/kg	Zn mg/kg
0-14	1.26	0.04	2.67	0.01	12.27	0.01	0.05	0.30
14-28	0.94	0.03	3.66	0.01	10.32	0.01	0.03	0.18

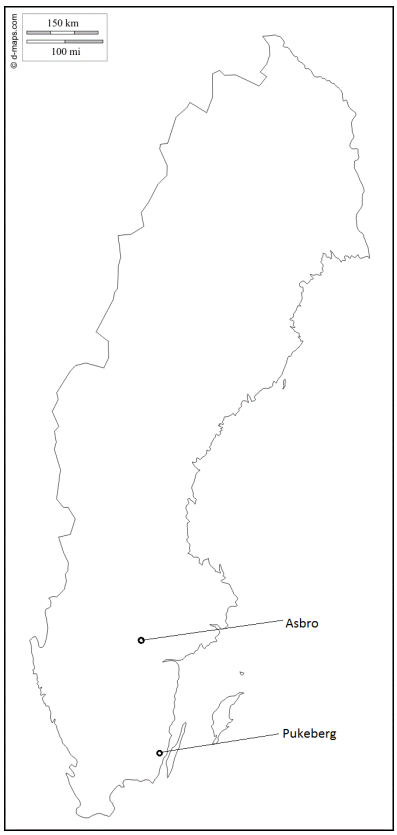

Figure 2 Location of the two examinated sites: Åsbro and Pukeberg

3.2 Titration curve

A titration curve was constructed with the purpose of finding out how much acid/base needed to be added to the soil to reach a specific pH value. The titration curve was performed on one column per site. For each column two layers with two replicates each were conducted. A 10 mM $NaNO_3$ solution was used as background solution with the purpose of assuring a relatively small range of ionic strengths in the experiment. To produce solutions of different acidity 2 g of field-moist soil was mixed with 19 ml H_2O (MilliQ), 10 ml of 30 mM $NaNO_3$ and either 1 ml HNO_3 or NaOH of different concentrations. NaOH was added in 3 different concentrations: 0.5 mM, 1 mM and 3 mM. On the other hand, HNO_3 was added in 11 different concentrations: 0 mM, 0.5 mM, 1 mM, 3 mM, 5 mM, 7 mM, 10 mM, 15 mM, 20 mM, 25 mM and 30 mM. Afterwards, the solutions were shaken in an end-over-end shaker for 3 days, and then centrifuged for 20 min at 2500 rpm. The supernatant of the centrifuged sample was collected and its pH was measured.

After the pH measurement the results were plotted as HNO_3/NaOH concentration vs. pH. An interpolation was conducted between the data points, to estimate how much acid or base was needed to get a specific pH. Based on these data a recipe for the batch test could be produced.

3.3 Batch test

All centrifuge tubes for the batch experiment and additionally all containers and filters for the metal analysis were acid washed before the experiments.

The batch test was performed in 110 ml centrifuge tubes. 6.667 g field moist soil, 79 ml H_2O (MilliQ), 20 ml $NaNO_3$ (concentration: 10 mM), and 1 ml HNO_3/NaOH in different concentrations were added. Again for each site two layers with two replicates each were conducted.

The samples were shaken in an end-over-end shaker. Different series of samples were produced, which were shaken for 1 day, 5 days or 30 days, respectively.

For 1-day and 30-days, suspensions with natural pH and low pH (for Pukeberg pH 4, for Åsbro pH 2.3/2.4), for 5-days suspensions with all pH values according to the recipe (Appendix) were mixed and subsequently analysed as described in the following section.

After shaking, the samples were centrifuged at 2500 rpm for 20min. A small amount (1 ml) of the supernatant was removed, to measure the pH value. The rest of the supernatant was filtered through 0,45 µm membrane syringe filters and then used for different analyses (Metalanalysis, Organic Carbon analysis).

20 ml of the filtered solution was filtered through 10 kDa ultracentrifuge filters at 2500 rpm for 20 min. The centrifuge filtration was repeated if there was more than 1 ml left of the retentate in the centrifuge tube above the filter.

The remaining ca. 20 ml was subject to PO_4^{3-} analysis. PO_4^{3-} was determined using a spectrophotometer. For the natural pH samples shaken for 5 days a full anion analysis was performed.

3.4 Dry weight

Around 40 g of the field moist soil sample was dried at 40°C for about 24 h.

The dry weight was calculated according to the following equation:

$$DW = \frac{m3 - m1}{m2 - m1}$$

DW	dry weight
m1	weight of bowl
m2	weight of field moist sample + bowl
m3	weight of dried sample + bowl

3.5 Extractions

3.5.1 Oxalate extraction

The oxalate extraction is often used to estimate the content of Fe and Al short-range-order minerals in soils (del Campillo, et al., 1992). The oxalate extracts all surface-reactive Al, while for Fe it mainly extracts ferrihydrite.

For each site two layers with two replicates each were conducted. 1 g dried soil sample was mixed with 100 ml 0.2 M oxalate solution (pH 3). The samples were shaken on a table shaker for 4 h in the dark (to prevent photochemically induced dissolution of crystalline Fe phases).

Afterwards, the samples were centrifuged at 4000 rpm for 15min and the supernatant sent to the ALS laboratory where the analysis was performed.

3.5.2 Geochemically active available fraction

For each site two layers with two replicates each were conducted. 1 g dried soil was mixed with 30 ml 0.1 M HNO_3. The solution were shaken in an end-over-end shaker for 16 h. Afterwards, the sample was centrifuged at 2500 rpm for 20 min and filtered through a 0.45 µm membrane syringe filter. The filtered samples were sent to the ALS laboratory for metal analysis.

3.6 Visual MINTEQ modelling

Visual MINTEQ 3.1 was used in an attempt to reconstruct the results received from the batch experiment. In the modelling attempt sorption to iron- and aluminium (hydr)oxides, binding to SOM, and dissolution/precipitation of minerals were included (Tiberg et al. 2016). The concentrations entered were based on chemical analyses. According to Tiberg et al. (2016), a Three Plane CD-Music model was used (Ferrih-CDM), in which both iron and aluminium (hydr)oxide are assumed to behave as ferrihydrite. Moreover, in this model the charge of the Stern layer is distributed over two electrostatic planes, according to an assumed structure of the surface complexes (Tiberg et al. 2016). SOM parameters were added using the SHM (Stockholm Humic model) model (Gustafsson 2001). Ferrihydrite (aged) and $Al(OH)_3$(soil) were entered into the model as possible soild phases, and are thereby formed if their saturation indices are smaller 1 (Tiberg et al. 2016). If formed, they control the activity of Fe^{3+} and Al^{3+} in solution (Tiberg et al. 2016). The temperature was adjusted to 21°C.

Model input:

- Geochemically active arsenic, as extracted by oxalate/oxalic acid
- Concentration of Na^+ and NO_3^- as added for each pH value
- DOC and PO_4^{3-} as determined for each pH value
- Ca, Mg, K, Fe, Al as determined for each pH value
- For Åsbro:
    - Pb, Cr, Cu and Zn as determined for each pH value
    - Ba und Mn: geochemically active concentrations as extracted by 0.1 mol/L HNO_3
- For Pukeberg:
    - Ba, Mn, Pb, Cr, Cu and Zn: geochemichally active concentrations, as extracted by 0.1 mol/L HNO_3
- It was assumed that the concentration of active SOM (consistent of 50% humic acid (HA) and 50% fulvic acid (FA)) accounts for 50% of the total organic matter. The organic matter, on the other hand, consisted of 50% C by weight (Tiberg et al. 2016)

- It was assumed that DOM consists of 100% FA, furthermore, the ratio of DOM to DOC was set to 2 (Tiberg et al. 2016)
- Ferrihydrite, used in the Three Plane CD-Music model, was entered as the sum of Fe and Al as extracted by oxalate/oxalic acid

4 Results

4.1 Experimental results

The results of the As K-edge EXAFS spectrum of both soils and both layers from the research project (Sjöstedt, pers. comm.) show that in both soils arsenic was mainly found as arsenate (As(V)). In general it can be said, that on both sites, but with different extent, the amount of dissolved arsenic is increasing with decreasing pH values for pH < neutral pH.

Figure 3 shows the arsenic solubility concentration as a function of pH for the Åsbro site. The natural pH for the Åsbro top layer (4-17 cm) was 6.1, whereas it was 6.7 for the bottom layer (17-30 cm). For pH values lower than natural pH the concentration of dissolved arsenic in the solution increased with decreasing pH (and therefore with increasing amount of added HNO_3) for both layers. For the pH value above the natural pH the amount of dissolved arsenic was about constant (4-17 cm) or increased slightly (17-30 cm).

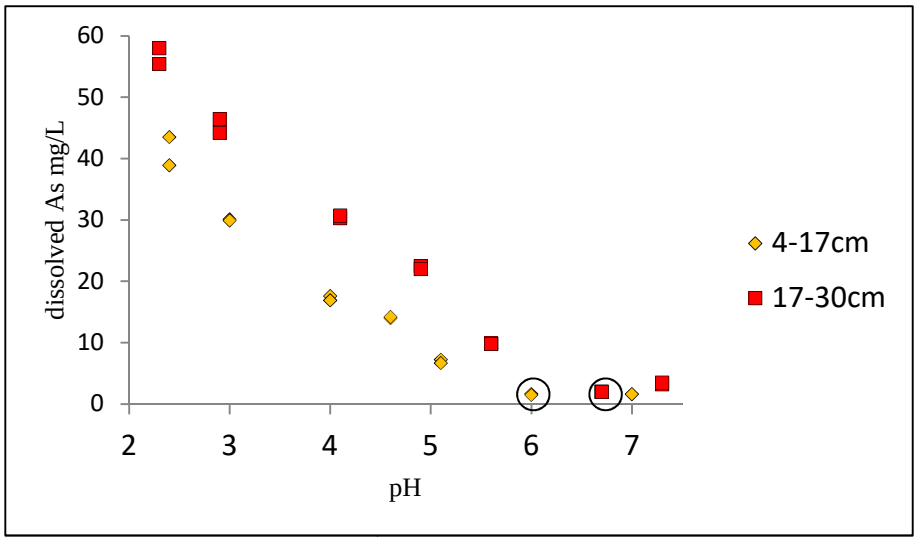

Figure 3 Dissolved arsenic (mg/L) as a function of pH for the Åsbro soil top and bottom layers. The circles show the samples to which no acid or base additions were made.

A similar behaviour can be seen for the Pukeberg samples (Figure 4). However, the natural pH in this soil was pH 8.1, i.e. higher than for the Åsbro site. For pH values lower than the natural pH the concentration of dissolved arsenic first decreased with decreasing pH values until pH 7, and then dissolved arsenic increased for pH values lower than 6.

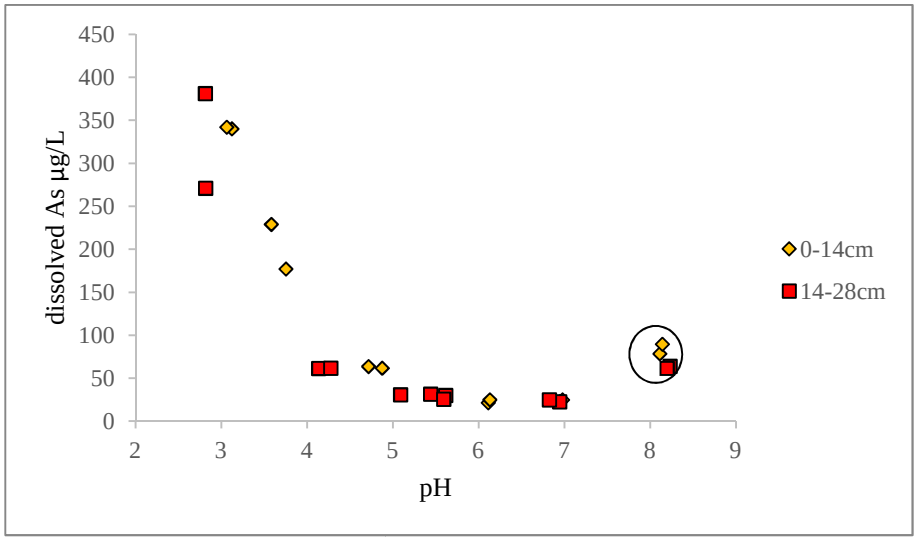

Figure 4 Arsenic solubility (µg/L) as a function of pH for the Pukeberg top and bottom layers. The circles show the samples to which no acid or base additions were made.

Figure 5 shows dissolved arsenic as a function of reaction time for the 4-17 cm and for 17-30 cm layers, measured for the samples without acid or base additions (final pH varied between 6.1 and 6.7). For Pukeberg the same is shown in Figure 6 (natural pH 8.1 for all samples). The figures show a similar behaviour for both soils, i.e. a slight increase in the concentration of dissolved arsenic from day 1 to day 5. For Åsbro the dissolved As concentration continued to increase slightly after day 5, whereas for Pukeberg dissolved As showed a slight decrease between 5 and 30 days.

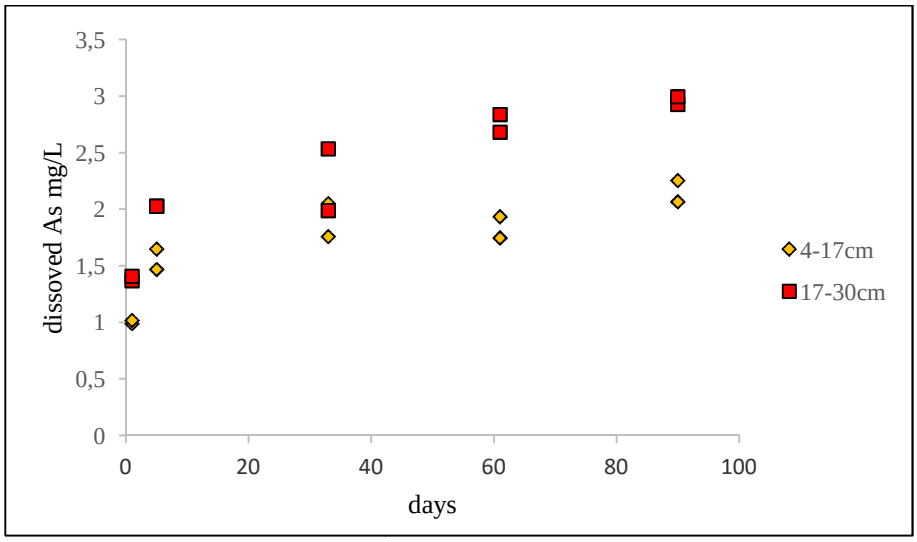

Figure 5 Arsenic solubility (mg/L) as a function of reaction time for the Åsbro top and bottom layers, for samples to which no acid or base had been added.

.

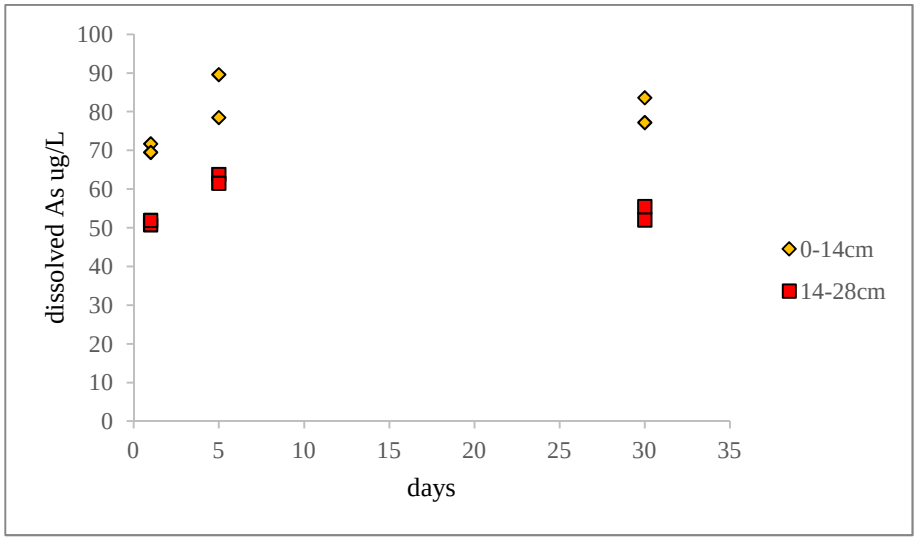

Figure 6 Arsenic solubility (µg/L) as a function of reaction time for the Pukeberg top and bottom layers, measured for samples to which no acid or base had been added.

Figure 7 and 8 show dissolved As as a function of reaction time, measured for the low pH samples (pH 2.3-2.4 in Åsbro and pH 4 in Pukeberg), to which 28-30 mmol/L HNO_3 in Åsbro and 10 mmol/L HNO_3 in Pukeberg 0-14 cm and 17 mmol/L HNO_3 in Pukeberg 14-28 cm had been added. Here, both soils showed the same behaviour: dissolved arsenic decreased with an increasing number of days of reaction. However, it should be noted that for both sites the measured pH value increased with an increasing number of days of reaction. This probably caused the observed effect on dissolved arsenic, as a decreased solubility of arsenic with increasing pH would be expected from the results shown in Figure 3 and Figure 4.

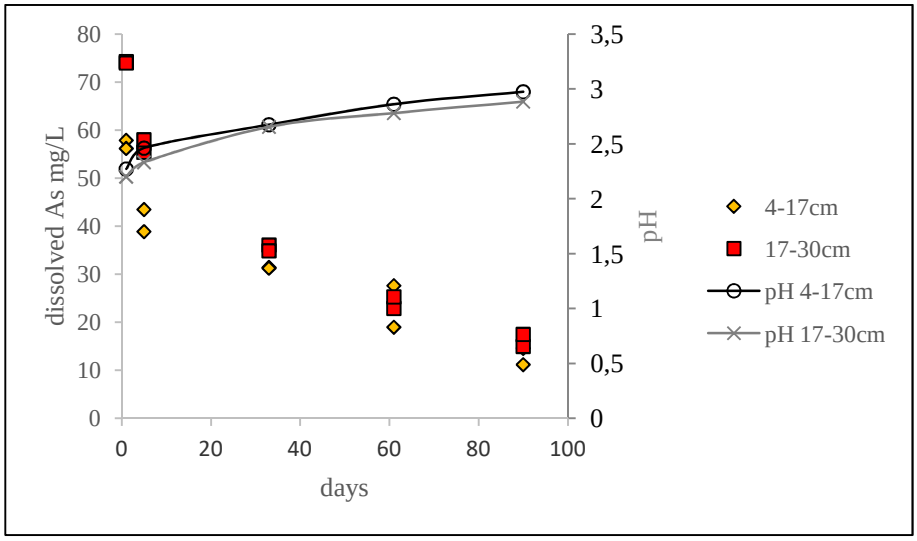

Figure 7 Arsenic solubility (mg/L) and pH variability as a function of reaction time for the Åsbro top and bottom layers, measured for samples to which 28-30 mmol/L HNO_3 had been added

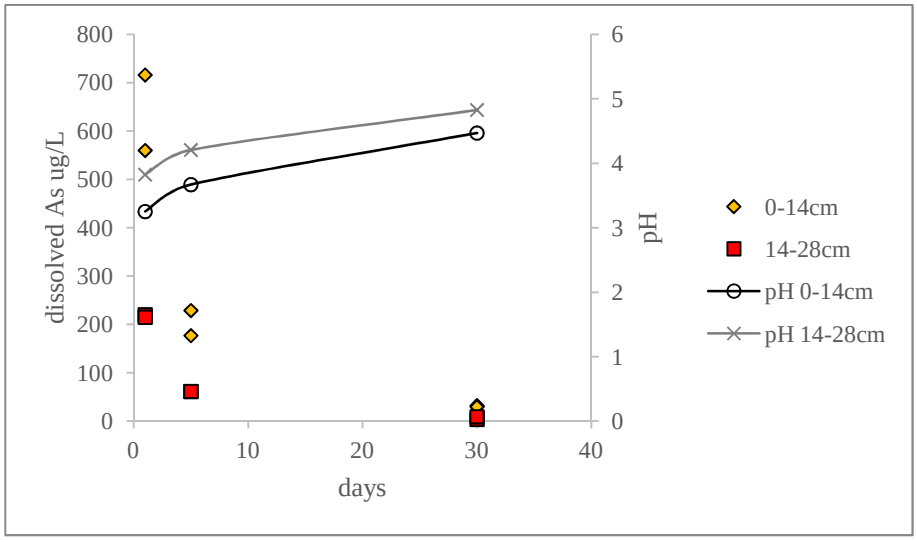

Figure 8 Arsenic solubility (µg/L) and pH variability as a function of reaction time for the Pukeberg top and bottom layers, measured for samples to which 17 mmol/L HNO_3 (top layers) and 10 mmol/L HNO3 (bottom layers) had been added

The pH dependence of the solubility of iron (Fe) was the same for both soils (Figure 9 and 10): the dissolved Fe was low and almost constant for high pH values, reflecting that almost all Fe was bound. At very low pH values, dissolved Fe increased strongly with decreasing pH. The only difference is that in the Åsbro soil Fe started to dissolve at pH 3, whereas in Pukeberg it started to dissolve at pH 4. The fact that Fe only dissolved at pH values lower than about 3-4 is consistent with Fe(III) being the predominant form of Fe, and that it was present mostly as ferrihydrite.

Dissolved iron was found in the same quantity in both soils, but the amount of dissolved Fe compared to other elements, and especially arsenic, in Åsbro was quite small. In Pukeberg on the other hand, the concentration of dissolved Fe exceeded the amount of dissolved arsenic at low pH values.

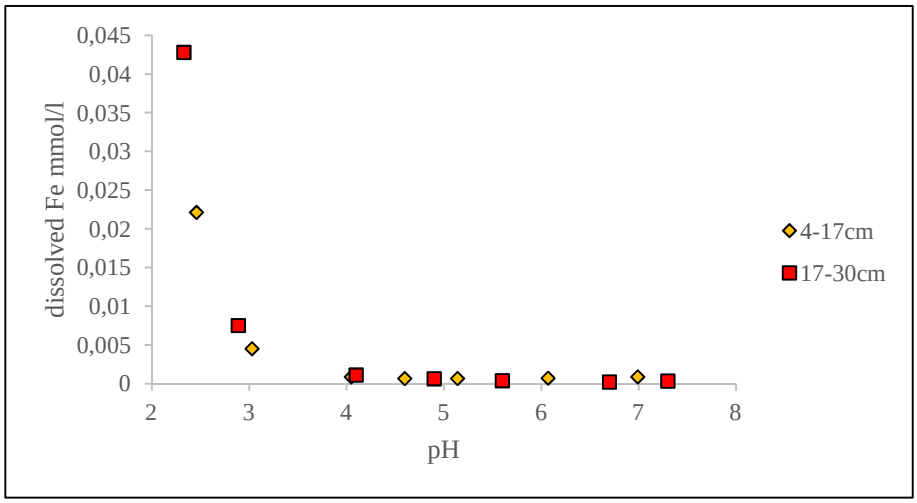

Figure 9 Solubility of iron (mmol/L) as a function of pH for the Åsbro top and bottom layers

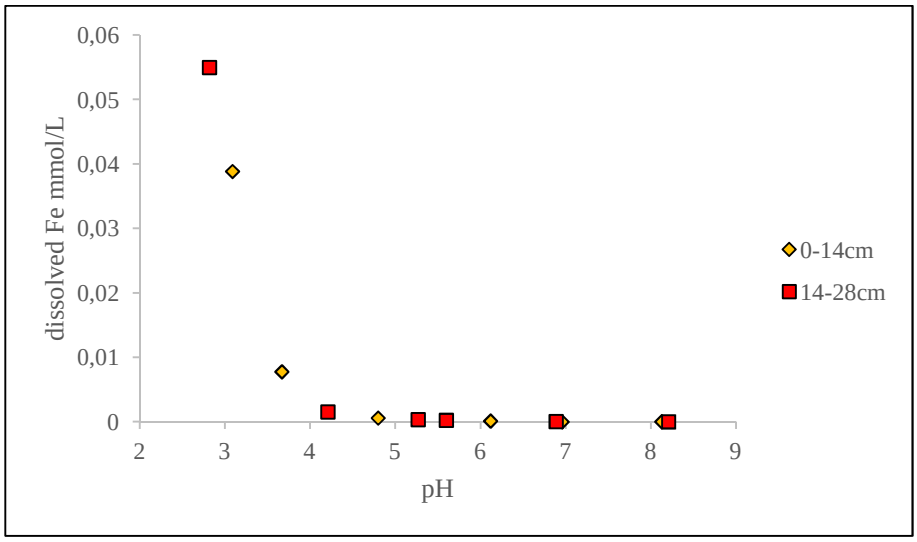

Figure 10 Solubility of iron (mmol/L) as a function of pH for the Pukeberg top and bottom layers

Aluminium had a similar pH-dependent solubility. Similar magnitudes of Al were dissolved at low pH in both sites (Figure 11 and 12). Again however, Pukeberg showed a higher Al solubility at higher pH values. For Åsbro, a difference between the top and bottom layers can be noticed: while the concentration of dissolved As increased already at pH < 5 for the bottom layer, Al only increased at pH < 4 in the top layer. This indicates that in the latter soil aluminium was probably not present as aluminium hydroxide (or some other hydroxyl-Al mineral phase), but possibly instead as organically bound Al. Geochemically active Al was 39.3 mmol/kg for the 4-17 cm and 32.3 mmol/kg for the 17-30 cm layer. This means that at pH 2.3 almost all geochemically active Al was dissolved.

For Pukeberg the amount of dissolved Al increased already at pH 6. This indicates the presence of a hydroxyl-Al mineral phase such as aluminium hydroxide.

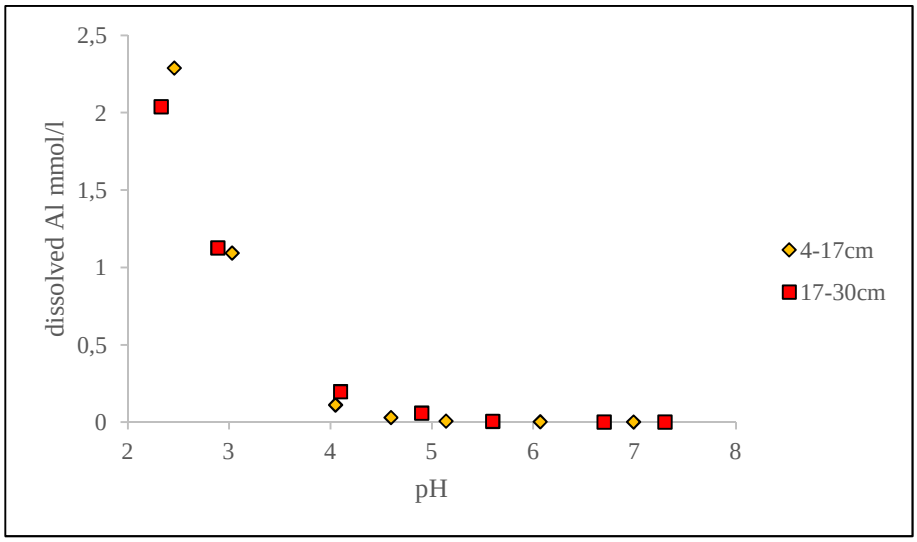

Figure 11 Solubility of aluminium (mmol/L) as a function of pH for the Åsbro top and bottom layers

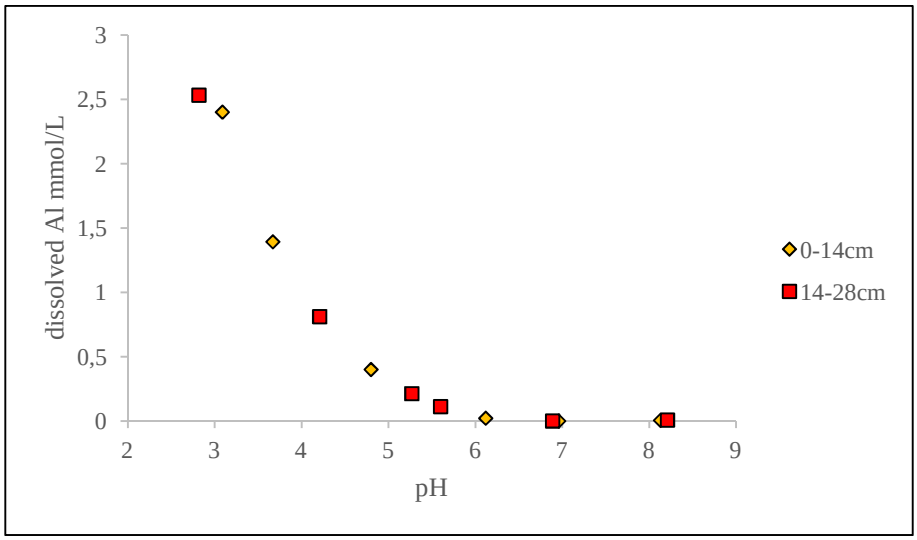

Figure 12 Solubility of aluminium (mmol/L) as a function of pH for the Pukeberg top and bottom layers

Figure 13 and Figure 14 show the pH-dependent solubility of other elements that might play a role in the binding of arsenic in the Åsbro site. Their pH-dependent solubility is compared to that of arsenic. Figure 13 shows the pH dependences for the top layer while Figure 14 shows the same for the bottom layer.

As for AsO_4^{3-}, PO_4^{3-} is an anion, and therefore a competitor for surface complex formation/ binding. As can be seen in Figure 13 andFigure 14, dissolved phosphate shows similar pH dependence as arsenic in both layers, i.e. an increased solubility with decreasing pH at pH values lower than the natural pH.

In both layers, the pH-dependent concentration of dissolved manganese was similar to that of arsenic. Possibly, manganese can play an important role in the binding of

arsenate either as an As-adsorbing Mn(III) or Mn(IV) oxide, or by precipitating arsenic as a Mn arsenate solid.

Magnesium is usually not thought of being of importance for the binding of arsenate, but for the bottom layer the similarity between dissolved Mg and dissolved arsenic was striking. This was, however, not true for the top layer.

According to some literature, Ca is believed to control the solubility of arsenic in calcium-dominated environments, especially if Fe/As ratios are low (Martinez-Villegas et al. 2013). The concentration of dissolved Ca in this soil was rather high, and similar to other cations, the dissolved Ca increased with decreasing pH; dissolved Ca was 3 times higher than that of Mg.

Additionally, in several cases Zn has been shown to be an accessible co-sorption partner for arsenic (Gräfe et al. 2008). In Åsbro Zn displayed a similar pH-dependent solubility as arsenic, but Zn was present at higher concentrations.

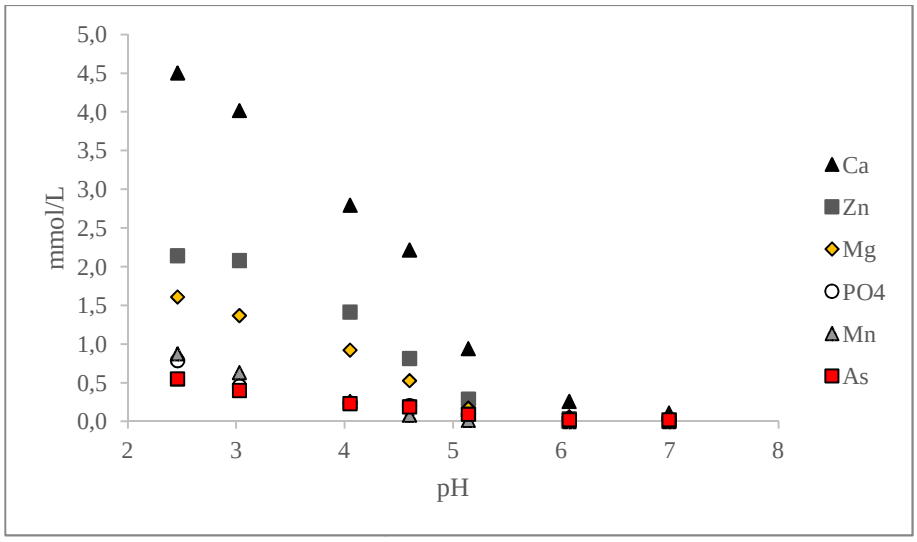

Figure 13 Solubility of Ca, Zn, Mg, PO_4, Mn and As as a function of pH for the Åsbro top layers

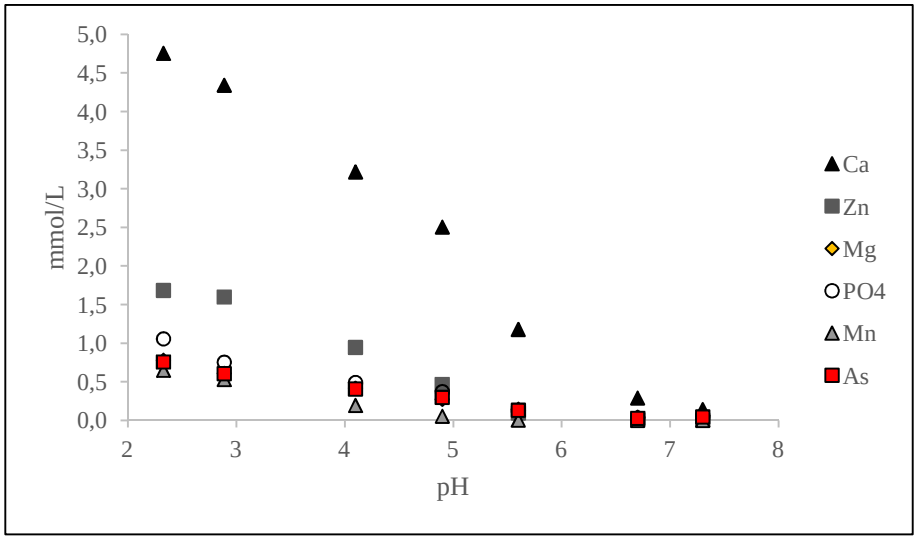

Figure 14 Solubility of Ca, Zn, Mg, PO_4, Mn and As as a function of pH for the Åsbro bottom layers

Figure 15 shows dissolved barium and lead for the Åsbro top and bottom layers as a function of pH. Compared to other elements, Ba and Pb were present only at low concentrations. Nevertheless dissolved Ba showed exactly the same pH-dependence as arsenic at pH < 6, whereas the solubility of Pb only increased with decreasing pH for pH values smaller than 4.

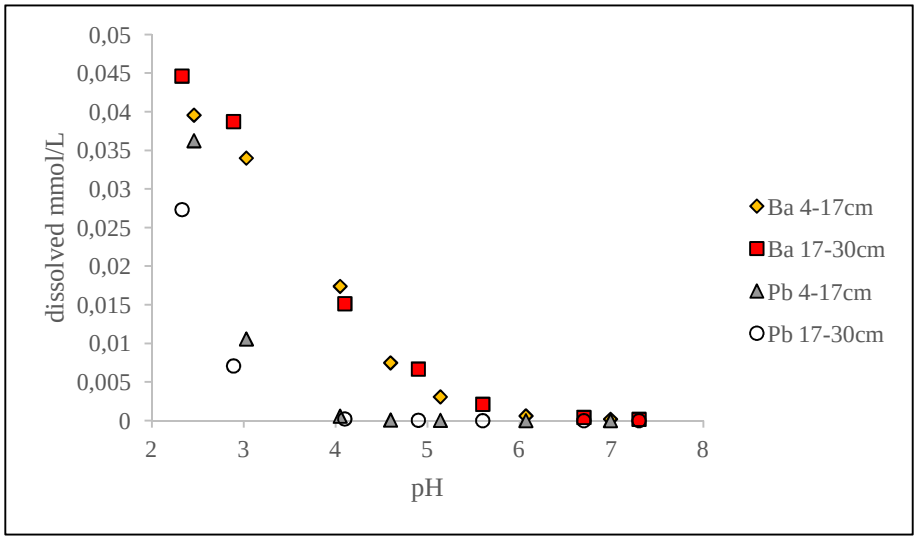

Figure 15 Ba and Pb solubility as a function of pH for the Åsbro top and bottom layers

Figure 16 and Figure 17 show the pH-dependent solubility of elements in the Pukeberg soil sample that might play a role in the surface complex formation and binding of arsenic. Figure 16 shows the amount of dissolved elements in the top layer as a function of pH, whereas Figure 17 shows the same for the bottom layer. A general observation is that all elements showed a similar pH-dependent behaviour.

Dissolved manganese and barium showed the least similarities to arsenic. Their dissolved concentrations increased steadily with decreasing pH for the whole pH range considered (3 to 8.1).

Even though lead and PO_4 showed a similar pH-dependent solubility as arsenic at pH < 5, both showed a pronounced increased solubility at low pH (more pronounced than that of As).

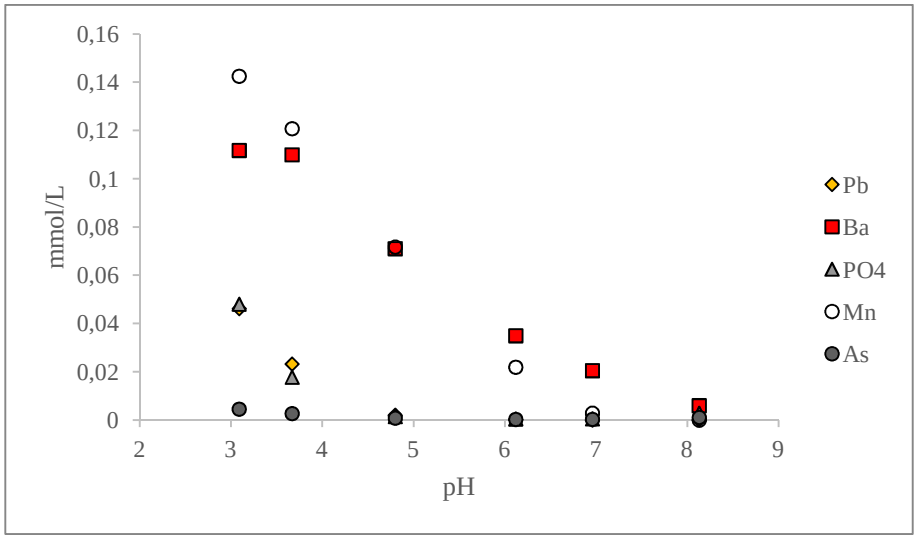

Figure 16 Dissolved Pb, Ba, PO_4, Mn and As as a function of pH for the Pukeberg top layers

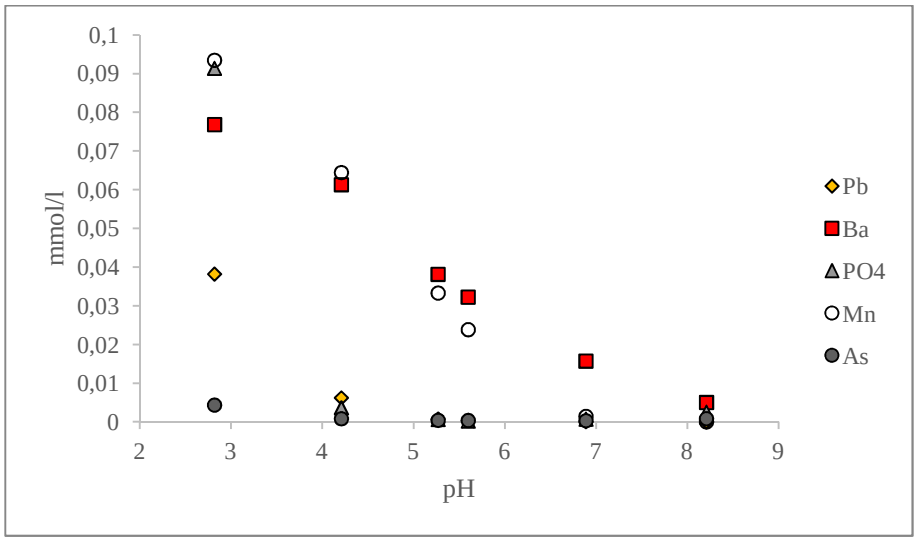

Figure 17 Dissolved Pb, Ba, PO_4, Mn and As as a function of pH for the Pukeberg bottom layers

4.2 Modelling results

4.2.1 Åsbro

Figure 18 andFigure 19 show dissolved arsenic as modelled with Visual MINTEQ compared to the results obtained from the batch test. In the modelling, arsenate was assumed to adsorb to ferrihydrite and Al hydroxide (when these were present), and in addition the precipitation of barium arsenate ($BaHAsO_4$:H_2O(s)) was allowed. The Ferrih-CDM (Tiberg et al. 2013) surface complexation model was used, the temperature was 21°C and the geochemically active values for barium and arsenic were used to constrain the total available concentrations in the system. This model deviated significantly from the experimental results, especially at higher pH. Therefore the saturation indices for several possible arsenic phases were investigated.

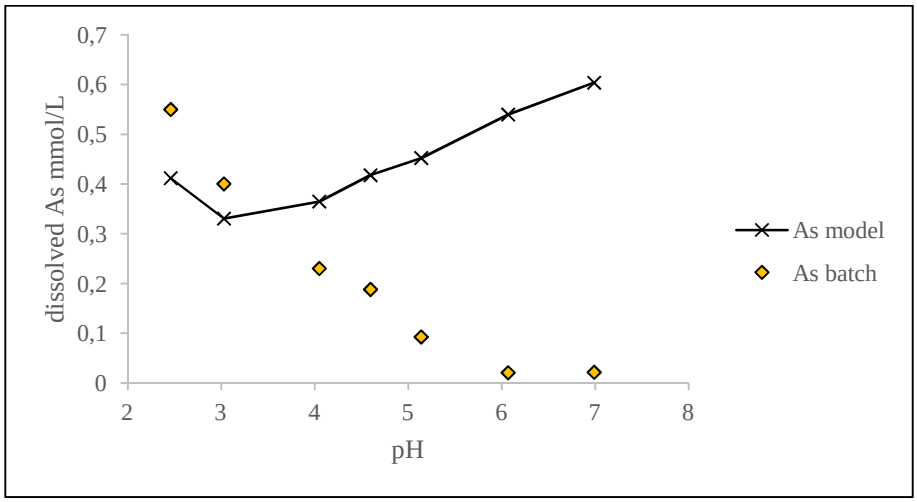

Figure 18 Surface complexation model with Ba-arsenate precipitation in Visual MINTEQ, compared to batch experiment results for the Åsbro top layers

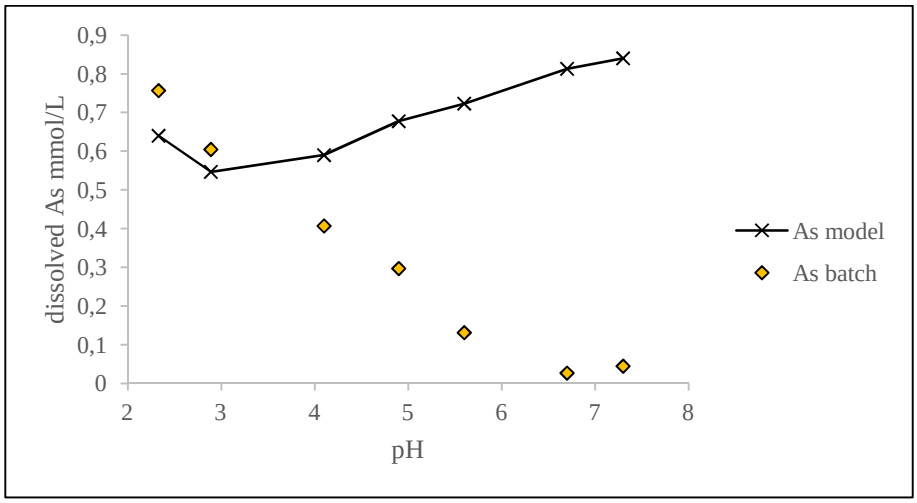

Figure 19 Surface complexation model with Ba-arsenate precipitation in Visual MINTEQ compared to batch experiment results for the Åsbro bottom layers

Figure 20 andFigure 21 show saturation indices for aluminium hydroxide, ferrihydrite and different arsenic phases for the Åsbro top and bottom layers. Ferrihydrite and $Al(OH)_3$ show only positive saturation indices for high pH values. However, a positive saturation index throughout almost the whole tested pH range was only found for the $BaHAsO_4$ precipitate. The other two phases ($MnHAsO_4$ and $CaHAsO_4$) show negative values for the whole pH range.

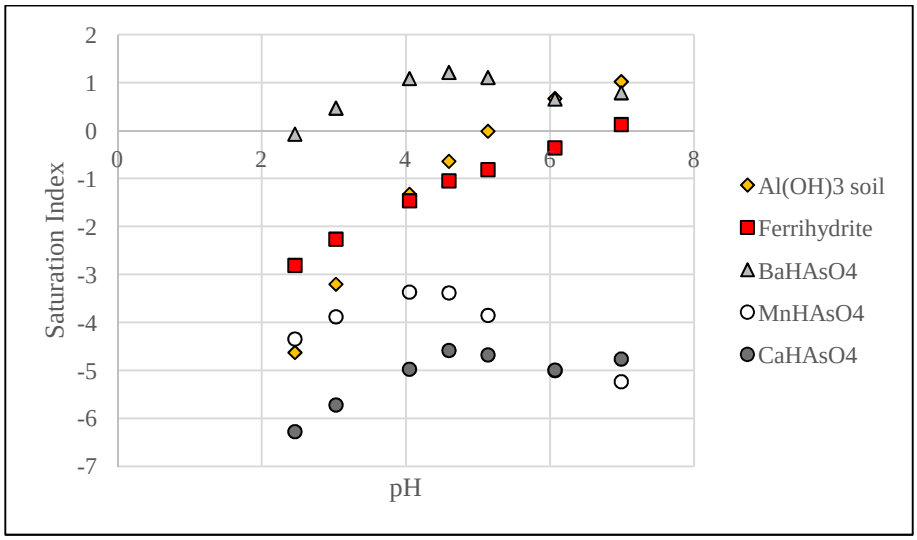

Figure 20 Saturation indices as a function of pH for $Al(OH)_3$, ferrihydrite, and the precipitates $BaHAsO_4$, $MnHAsO_4$ and $CaHAsO_4$ calculated using Visual MINTEQ for the Åsbro top layers

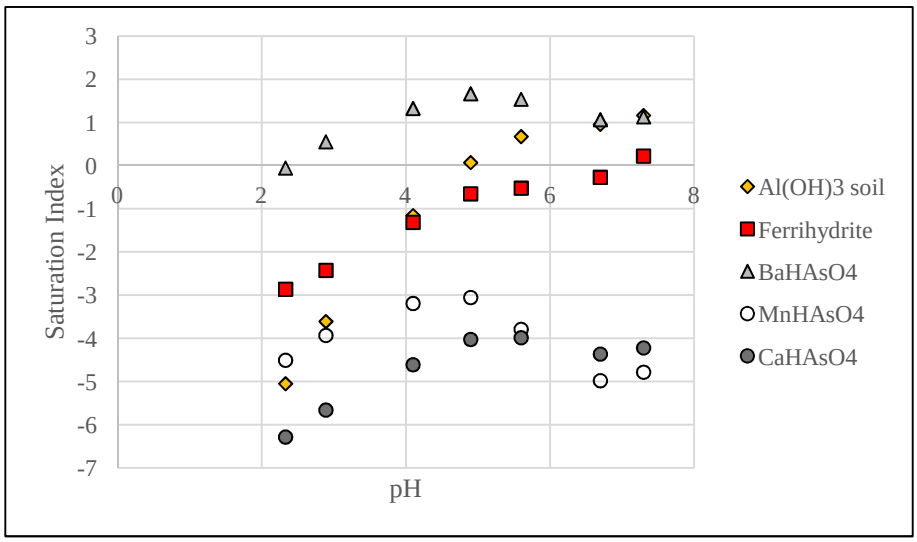

Figure 21 Saturation indices as a function of pH for $Al(OH)_3$, ferrihydrite, and the precipitates $BaHAsO_4$, $MnHAsO_4$ and $CaHAsO_4$ calculated using Visual MINTEQ for the Åsbro bottom layers

4.2.2 Pukeberg

Figure 22 and Figure 23 show the model fits for Pukeberg generated with Visual MINTEQ 3.1 compared to the results from the batch test. In this case the model was generated including SOM, inorganic C, corrected ferrihydrite values, PO_4^{3-} as determined for each pH value and geochemically active values for the following elements: Pb, Ba, Cr, Mn, Cu and Zn. The model also included possible equilibrium with $Al(OH)_3$ (soil) and ferrihydrite (aged). The surface complexation model "Ferrih-CDM (Tiberg et al. 2013)" was used. It should be noted that the y-axis of both graphs is in a logarithmic scale.

In general it can be said that the model and the experimental results showed a similar pH dependence, but that the simulated concentrations of dissolved arsenic differed strongly. The concentrations of dissolved arsenic in the model were much lower than the experimental results.

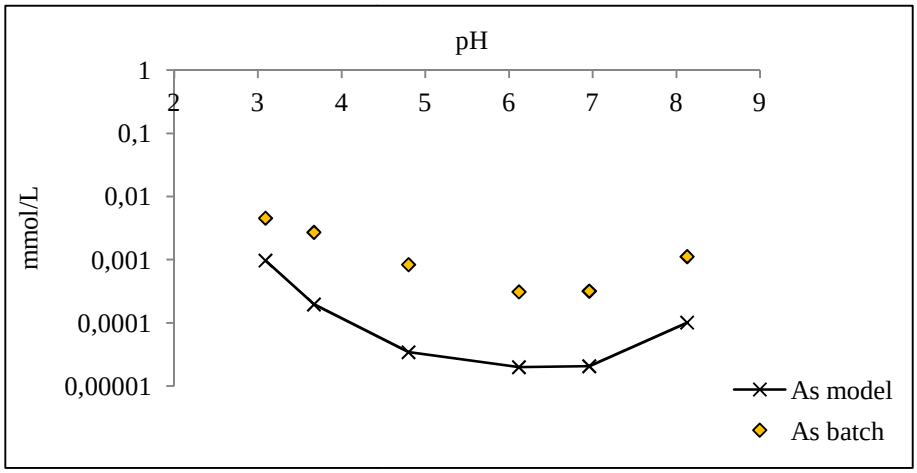

Figure 22 Surface complexation model (see text) compared to batch experiment results for the Pukeberg top layers

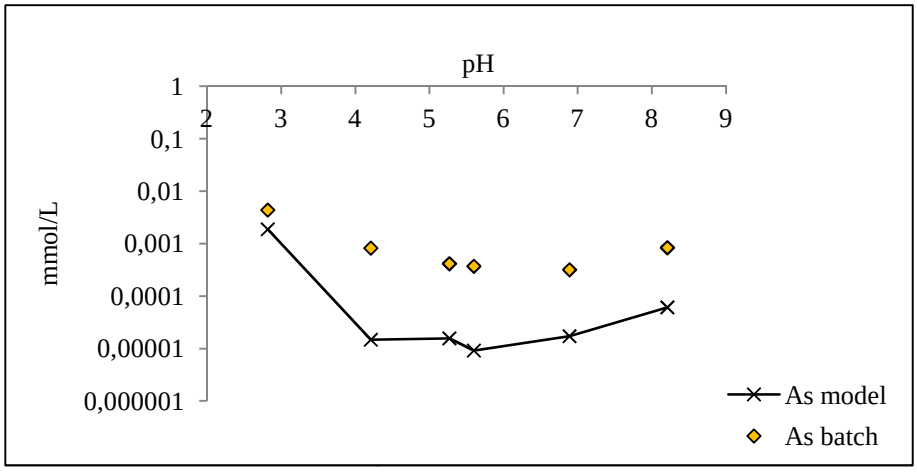

Figure 23 Surface complexation model (see text) compared to batch experiment results for the Pukeberg bottom layers

5 Discussion

The results on the solubility of arsenate as a function of pH are in disagreement with much of the previous literature. Generally, most authors have observed stable and high As(V) adsorption in the pH range of 3 to 8, an increase of arsenate solubility with increasing pH values at pH 8 and above, and increasing arsenate solubility with decreasing pH at pH 3 and below (Lumsdon et al. 2001; Pantsar-Kallio and Manninen 1997; Goldberg and Johnston 2001; Dankwarth and Gerth 2002; Williams et al. 2003; Burns et al. 2006; Bisone et al. 2016). In all these former experiments, arsenic sorption was thought to be governed by As(V) adsorption to Fe and Al (hyr)oxides. By contrast, in this experiment, the solubility of arsenic increased with decreasing pH already at pH values below 6 in Åsbro and pH 5 in Pukeberg.

A first presumption can be that equilibrating the soil for 5 days is not sufficient for the desorption of arsenic at equilibrium. However, this presumption can be refuted, as the experiments with different reaction times show stable or declining values of dissolved arsenic with an increasing number of days.

According to ongoing work in the research project (Sjöstedt, pers. comm.), the As K-edge EXAFS spectrum for the Åsbro top layer could be fitted with a model of arsenate adsorbed to about 40% amorphous aluminium hydroxide and 55% ferrihydrite. The spectrum of the bottom layer could be fitted with 80% ferrihydrite and 20% aluminium hydroxide. Nevertheless these results are preliminary and do not exclude the fact that other phases might be present in this soil.

However, the surface complexation model for Åsbro, containing ferrihydrite and $Al(OH)_3$ as possible adsorbent phases (Figure 18 Figure 19) showed similarities to the observations only for pH values between 2.3 and 3. Otherwise, there were great discrepancies with the batch experiment results. This indicates that, in this case, ferrihydrite and aluminium hydroxides might only play a limited role for arsenic binding and that other As-binding phases are probably involved as well.

The saturation indices show that ferrihydrite was undersaturated over almost the whole pH range. They are only close to 0 for the high pH values. This indicates that ferrihydrite is unstable at low pH, which may reduce the number of adsorption sites. Aluminium hydroxide on the other hand is saturated at a pH value around 5 and oversaturated for pH >5, and therefore probably available as an adsorbing mineral phase at these pH values.

The situation in Pukeberg is slightly different. In this case the surface complexation model was able to describe the pH dependence, but the model fit shows about 10 times less dissolved arsenic than the observations suggest. The experiment by Moldovan and Hendry (2005) showed similar results as the Pukeberg results, with a decreasing arsenic solubility with increasing pH up to 5 and a low solubility between pH 5 and pH 7.3

(Moldovan und Hendry 2005). In this former experiment, ferrihydrite was the dominant As adsorbent phase (99.8% of the total) throughout the pH range from 3.2 to 11 (Moldovan und Hendry 2005). Additionally, in the pH range from 5 to 8 the remaining 0.2% As was adsorbed to amorphous aluminium hydroxide (Moldovan und Hendry 2005).

Besides, the batch experiment results showed that the pH-dependent concentrations of dissolved aluminium (Figure 12) and arsenic correspond, with increasing concentrations at pH < 5. Aluminium is known to play an important role in the solubility of arsenic (Manning and Goldberg 1997; Goldberg 2002; Moldovan and Hendry 2005; Bissen and Frimmel 2003; Sadiq 1995). Nevertheless, it was shown by Goldberg, that arsenate adsorbs to 100% on amorphous Al oxides in a pH range 3-9 (Goldberg 2002), this indicates that the Al oxides are not the dominant adsorption sites in the Pukeberg soil samples. Al hydroxides on the other hand precipitate over the pH range 5-9 and show signs of arsenic adsorption starting at pH 5 with a maximum at pH 8 (Goldberg 2002). This was also confirmed by Manning and Goldberg (1997), who found arsenic adsorption to Aluminium hydroxides over the pH range 4-9 (Manning und Goldberg 1997). Therefore Al hydroxides are potentially to be considered as arsenate adsorption sites in this soil.

Concerning the Pukeberg sample there are different possible explanations for the fact that the pH dependence trend of the model but not the dissolved concentrations are in agreement with the observations. One reason could be related to the available adsorption sites in the soil. A possible explanation might be that a large part of the Fe and Al (hydr)oxides (which could function as adsorption sites), are situated inside bigger particles, and therefore not in direct contact with the arsenic. This in turn reduces the available adsorption sites. Therefore, Visual MINTEQ might assume a larger number of adsorption sites than actually available in the soil. Figure 24 and Figure 25 show a model attempt with a smaller number of adsorption sites. Therefore, the amount of ferrihydrite was reduced to 50and 25 % of the originally used amount. It can be seen that the 25 % ferrihydrite model is closest to the actual experimental results, which is consistent with this hypothesis; however, additional experiments would be needed for any direct evidence.

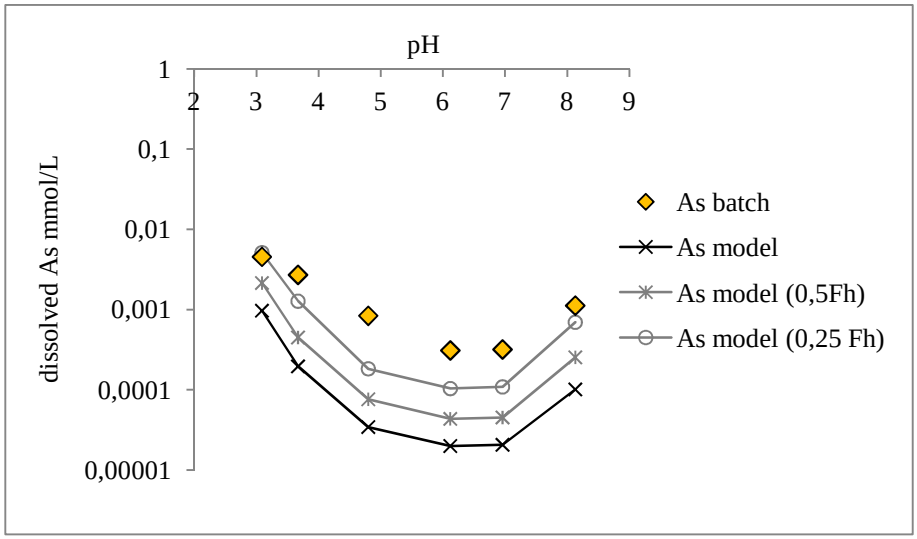

Figure 24 Dissolved arsenic from batch experiments compared to the surface complexation model, a model with 50 % ferrihydrite (0.5 Fh) and a model with 25% ferrihydrite (0.25 Fh) for the Pukeberg top layers

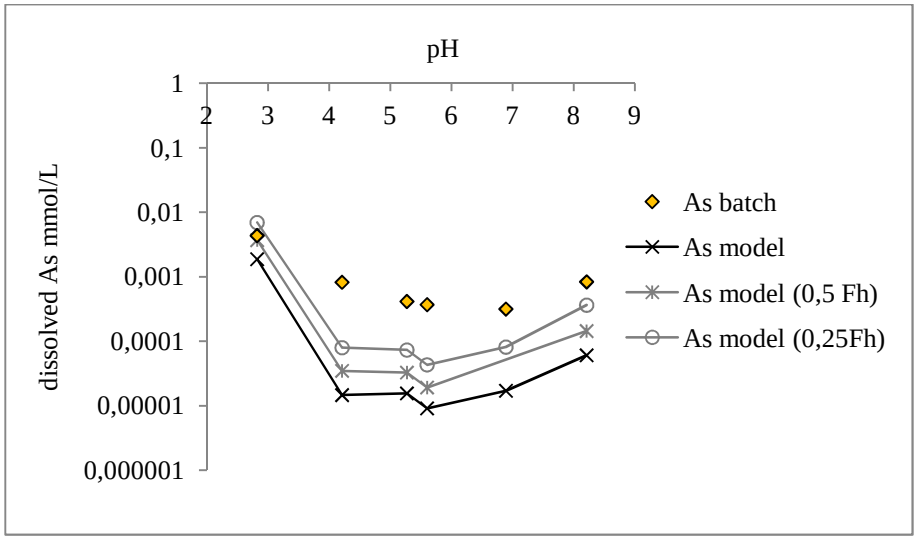

Figure 25 Dissolved arsenic from batch experiments compared to the surface complexation model, a model with 50 % ferrihydrite (0.5 Fh) and a model with 25% ferrihydrite (0.25 Fh) for the Pukeberg bottom layers

Given the finding that in the Åsbro soil ferrihydrite and aluminium hydroxide may not be the main phases controlling the arsenic release, other phases must be responsible for the binding of arsenic. Depending on the pH, the formation of metal-arsenate salts are possible if the Fe/As ratios are low (Martinez-Villegas et al. 2013; Villalobos et al. 2010).

For example, a similar As solubility behaviour as in Åsbro was shown in the investigations of Jang et al. (2002). They observed increasing concentrations of dissolved As with decreasing pH for pH < 6 (at pH 2, the arsenic concentration was close to the total concentration of arsenic present in the chromate copper arsenate-contaminated soil) and increasing dissolved As with increasing pH for pH > 6. It was suggested that arsenic leaching was caused by metal complexation with acetate rather

than simply by pH (Jang et al. 2002). But available data for Åsbro is inconclusive whether CCA was applied in the area or not, information is only given on the use of salts of copper, chromium and arsenic (Jernlås and Karlgren 2009).

Another explanation might be the formation of calcium arsenates. Nevertheless, calcium arsenates are more soluble than other metal arsenates (Martinez-Villegas et al. 2013; Villalobos et al. 2010). Martinez et al. (2013) showed that in contact with water arsenic and calcium were readily released into the investigated soils, especially in the more polluted, acidic and oxidised sites. This is also supported by Villalobos et al. (2010), who showed that the Ca arsenates were dissolved at pH < 8 and that they only precipitate at high pH values. Román-Ross et al. (2006) showed that carbonate minerals may adsorb arsenic in the pH range 7-9. Calcium is present in large amounts in Åsbro, but as Ca-As(V) precipitates are only stable at high pH they are unlikely candidates for the arsenic solubility behaviour in this soil. Furthermore, the saturation indices for the $CaHAsO_4$ phase show that undersaturation prevailed throughout the whole pH range, and is therefore unlikely to exist.

In addition, Zn has been mentioned by several authors as a possible precipitation partner of arsenate. In Figure 13 and Figure 14 it can be seen that the Åsbro soil contained relatively high concentrations of dissolved Zn. According to Gräfe et al. (2004) co-sorption of Zn and As(V) on goethite plays an important role. Their results showed that without the presence of Zn the adsorption of As(V) to Zn was already greater at pH 7 than at pH 4, but in the presence of Zn, the sorption of arsenate increased even more, by 29% at pH 4 and by 500% at pH 7 (Gräfe et al. 2004). In this experiment the adsorption of arsenic was weak at pH 4. Hence there is no direct evidence for co-sorption with Zn being a key process of arsenic adsorption in the Åsbro soil. Furthermore the geochemical model gives also no indications of saturation with respect to Zn arsenates.

As lead arsenate was formerly used in arsenical insecticides, several investigations on the stability of lead arsenate have been made. There are several different known lead arsenates with different pH values at which they precipitate, varying from low pH values (schultenite ($PbHAsO_4$)) to high pH values ($Pb_8As_2O_{13}$) (Magalhaes and Silva 2003; Liu et al. 2009; Gutiérrez-Ruiz et al. 2012). In general, the solubility of lead arsenates is known to be high, even though Magalhaes and Silva (2003) mentioned mimetite as a very stable lead arsenate. Moreover, the formation of a mixture of $PbHAsO_4$:H_2O and $Pb_3(AsO_4)_2$ precipitating at pH 6,5 was shown by Liu et al. (2009). Gutiérre-Ruiz et al. (2012) showed that in most of their samples, duftite ($PbCu(AsO_4)OH$) and hydroxymimetite ($Pb_5(AsO_4)_3OH$) coexisted at a pH range of 5.5 to 9.5. These conditions are relevant for the Åsbro soil. However, lead is present only in small amounts in Åsbro, and can therefore also not be responsible for the behaviour of As(V).

The only precipitate that was indicated by Visual MINTEQ to be of possible significance was barium arsenate ($BaHAsO_4*H_2O$). This can, for example, be seen in the saturation indices, where the $BaHAsO_4$ phase shows oversaturation through the whole pH range. It was shown by Zhu et al. (2005) that barium arsenate precipitates within the pH range of 3.6 to 7.4, with increasing solubility at lower pH and increasing stability at increasing pH values. However, the concentration of dissolved Ba in the Åsbro soil was very small (Figure 15) and therefore it is probably not responsible for the behaviour of arsenic solubility to a large extent.

In Figure 16 and Figure 17, it can be seen that the Pukeberg soil samples contained high concentrations of dissolved Ba and Pb. However, it seems that Pb and Ba did not play a crucial role in the binding of arsenic in this soil. A model including a $BaHAsO_4$ solid was compared to the model without this solid (Figure 26), showing that both models were in accordance except at high pH values, where the model including the solid deviated even more from the batch experiment results.

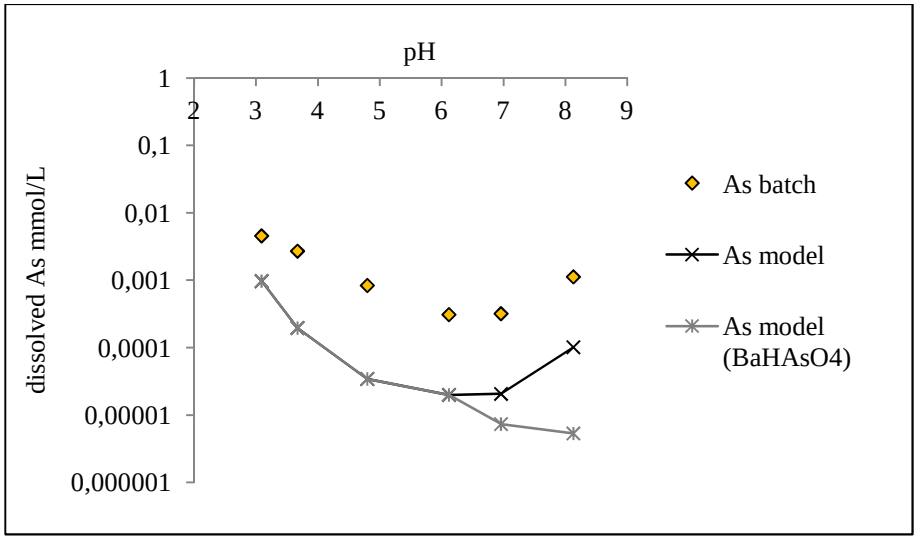

Figure 26 Dissolved arsenic from batch experiments compared to the surface complexation model (As model) and a model including $BaHAsO_4$ as possible solid phase for the Pukebrg top layers

There are several reasons why Mn oxides are known to be important minerals in soil: First, Mn oxides have a widespread distribution. Second, they have a high reactivity with high sorption capacities (Fischel et al. 2015). Many authors mention Mn oxides as an adsorbent phase for arsenate (Deschamps et al. 2003; Fischel et al. 2015). For these reasons, synthetic birnessite (MnO_2), which is often seen as a representative of many natural occurring manganese oxides, has been investigated by several authors (Manning et al. 2002). It is well known that Mn oxide plays an important role in the oxidation of As(III) to As(V) (Fischel et al. 2015; Deschamps et al. 2003; Manning et al. 2002; Moore 1990; Tournassat et al. 2002). It was shown that the oxidation of As(III) to As(V) is a two-step process, in which the actual oxidation occurs in the first step, while

in a second step the released As(V) forms low-solubility manganese-arsenic precipitates, similar to $Mn_3(AsO_4)_2$ and/or a compound similar to krautite ($MnHAsO_4{:}H_2O$) (Manning et al. 2002; Moore 1990; Tournassat et al. 2002). This two-step process is delineated in the formulas underneath:

(1) $2MnO_2 + H_2AsO_3 + H_2O = 2MnOOH + H_3AsO_4$

(2) $2MnOOH + H_3AsO_3 + 4H^+ = 2Mn_2+ + H_3AsO_4 + 2\ H_2O$

(3) $Mn^{2+} + H_2AsO_4^- + H_20 = MnHAsO_4{:}H_20 + H^+$

Manning et al. (2002) on the other hand described the adsorption of As(V) as adsorption to the MnO_2 surface (Manning et al. 2002). Mn-OH in the below-mentioned formula represents a reactive hydroxyl group on the MnO_2 surface (Manning et al. 2002)-

(4) $2Mn\text{-}OH + H_3AsO_4 = MnHAsO_4 + H_2O$

Figure 13 and Figure 14 show a relatively high Mn content of the soil, which exceeds the Fe content by far (Figure 9). Nevertheless, according to the saturation indices for $MnHAsO_4$ (Figure 20 Figure 21) in the Åsbro top and bottom layers, this precipitate was undersaturated at all tested pH values, and would therefore most probably not form. However, in the Åsbro soil, PO_4 and arsenic show the same solubility behaviour. According to the saturation index for $MnHPO_4$ (Figure 27), this precipitate is oversaturated over the whole tested pH range. As $PO_4^{3-}$and AsO_4^{3-} are both anions, and therefore known to behave similarly, it is difficult to completely rule out the formation of $MnHAsO_4$ as a possibility.

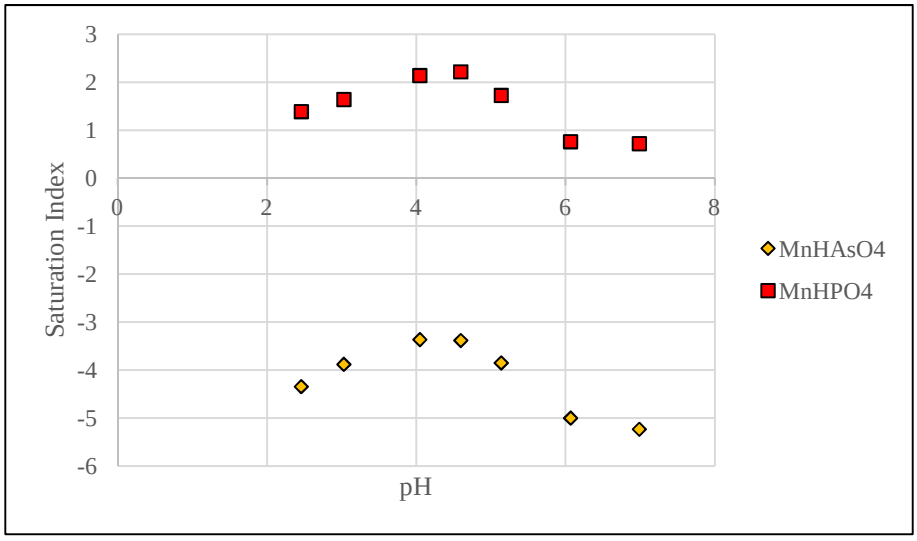

Figure 27 Saturation indices as a function of pH for $MnHAsO_4$ and $MnHPO_4$ calculated with the help of Visual MINTEQ for the Åsbro top layers

As was already mentioned in the results section, magnesium and arsenate had similar dissolved concentrations in the Åsbro bottom layer. This might suggest some kind of

binding between magnesium and arsenate. Because Mg usually does not play a major role in the adsorption of arsenate, there is not much information about magnesium arsenates in the literature. Nevertheless the occurrence of hoernesite ($Mg_3(AsO_4)_2*8H_2O$) has been mentioned by Voigt et al. (1996), but hoernesite is usually found with other arsenates and phosphates in highly altered rocks and in As-containing ore deposits. None of these situations apply to Åsbro. Furthermore, there is not much data available concerning the solubility of hoernesite. Hence, the formation of some kind of magnesium arsenate, maybe together with other metal ions, cannot be entirely excluded.

To model the adsorption of As, it is necessary to identify reactive solid phases in the contaminated soil beforehand, and to have an appropriate database containing metal surface complexation constants (Lumsdon et al. 2001). The results of this study confirm this assumption, as the models could not be adjusted to the batch experiment results. Without experiments revealing more details about the chemistry of the soil and information about solid reactive phases present, no clear statement or explanation on the fact that arsenic was not bound strongly in this soil can be given.

In general, under today's soil conditions the leaching of arsenic from both areas (Åsbro and Pukeberg) are not likely to be a problem, but if these conditions change, especially a change in the pH of the soil, the situation might change and arsenic leaching might become a greater problem. Following research on methods of removing arsenic from contaminated soils or surface waters should be considered on both sites in order to prevent future leaching of arsenic from the soil and subsequent contamination of drinking water sources.

6 Conclusion

This study showed, that for Åsbro, in contrary to earlier expectations, ferric (hydr)oxides were not the main governing adsorption sites. For Pukeberg, no explicit statement on the role of ferric (hydr)oxides as adsorption sites for As can be made. Furthermore, the assumption that arsenic adsorption results in a low leachability of As for pH above 3 was disproven, especially for the Åsbro area site.

For the Åsbro site, the results suggest the involvement of Mn-As precipitates, and/or metal arsenates influencing the solubility of As in the soil, while for Pukeberg the involvement of aluminium hydroxides is more likely. But without further characterization of the soil and existing reactive solid phases, an explicit statement on the arsenic sorption mechanisms cannot be given. Hence with the used approach it was not possible to adjust the geochemical model to the batch experiment results. Thus the lack of detailed characterisation constitutes a limiting factor for the use of geochemical modelling in risk assessment.

Additionally, the results indicate that a change in the soil pH might have a great influence on arsenic adsorption in both soils, and arsenic leaching might become a great problem.

7 References

Akter, Kazi Farzana; Owens, Gary; Davey, David E.; Naidu, Ravi (2005): Arsenic Speciation and Toxicity in Biological Systems 184, S. 97–149. DOI: 10.1007/0-387-27565-7_3.

Bisone, Sara; Chatain, Vincent; Blanc, Denise; Gautier, Mathieu; Bayard, Rémy; Sanchez, Florence; Gourdon, Rémy (2016): Geochemical characterization and modeling of arsenic behavior in a highly contaminated mining soil. In: *Environ Earth Sci* 75 (4). DOI: 10.1007/s12665-015-5203-z.

Bissen, Monique; Frimmel, Fritz H. (2003): Arsenic — a Review. Part I. Occurrence, Toxicity, Speciation, Mobility. In: *Acta hydrochim. hydrobiol.* 31 (1), S. 9–18. DOI: 10.1002/aheh.200390025.

Burns, Perre E.; Hyun, Seunghun; Lee, Linda S.; Murarka, Ishwar (2006): Characterizing As(III,V) adsorption by soils surrounding ash disposal facilities. In: *Chemosphere* 63 (11), S. 1879–1891. DOI: 10.1016/j.chemosphere.2005.10.026.

Chien, Shui-Wen Chang; Chen, Shou-Hung; Geethangili, Madamanchi; Huang, H. B. (2012): Adsoption Characteristics of Aqueous Arsenic(III) and Arsenic(V) in Taiwan Soils. In: *International Journal of Applied Science and Engineering* 10 (4), S. 333–344. DOI: 10.1002/9781118170229.ch1.

Dankwarth, Franka; Gerth, Joachim (2002): Abschätzung und Beeinflussbarkeit der Arsenmobilität in kontaminierten Böden. In: *CLEAN – Soil, Air, Water* 30 (1), S. 41–48. DOI: 10.1002/1521-401X(200207)30:1<41::AID-AHEH41>3.0.CO;2-1.

Deschamps, Eleonora; Ciminelli, Virginia S. T.; Weidler, Peter G.; Ramos, Aline Y. (2003): Arsenic sorption onto soils enriched in Mn and Fe minerals. In: *Clays and Clay Minerals* 51 (2), S. 197–204. DOI: 10.1346/CCMN.2003.0510210.

Dousova, Barbora; Buzek, Frantisek; Lhotka, Miloslav; Krejcova, Stanislava; Boubinova, Radka (2016): Leaching effect on arsenic mobility in agricultural soils. In: *Journal of hazardous materials* 307, S. 231–239. DOI: 10.1016/j.jhazmat.2015.12.030.

Elert, Mark; Höglund, Lars Olof (2012): Huvudstudie Pukebergs Glasbruk. Kemakta Konsult AB.

Fischel, Matthew H. H.; Fischel, Jason S.; Lafferty, Brandon J.; Sparks, Donald L. (2015): The influence of environmental conditions on kinetics of arsenite oxidation by manganese-oxides. In: *Geochemical transactions* 16, S. 15. DOI: 10.1186/s12932-015-0030-4.

Goldberg, Sabine (2002): Competitive Adsorption of Arsenate and Arsenite on Oxides and Clay Minerals. In: *Soil Science Society of America Journal* 66 (2), S. 413. DOI: 10.2136/sssaj2002.4130.

Goldberg, Sabine; Johnston, Cliff T. (2001): Mechanisms of Arsenic Adsorption on Amorphous Oxides Evaluated Using Macroscopic Measurements, Vibrational Spectroscopy, and Surface Complexation Modeling. In: *Journal of colloid and interface science* 234 (1), S. 204–216. DOI: 10.1006/jcis.2000.7295.

Gräfe, Markus; Nachtegaal, Maarten; Sparks, Donald L. (2004): Formation of Metal−Arsenate Precipitates at the Goethite−Water Interface. In: *Environ. Sci. Technol.* 38 (24), S. 6561–6570. DOI: 10.1021/es035166p.

Gräfe, Markus; Tappero, Ryan V.; Marcus, Matthew A.; Sparks, Donald L. (2008): Arsenic speciation in multiple metal environments II. Micro-spectroscopic investigation of a CCA contaminated soil. In: *Journal of colloid and interface science* 321 (1), S. 1–20. DOI: 10.1016/j.jcis.2008.01.033.

Gustafsson, Jon Petter (2001): Modeling the Acid–Base Properties and Metal Complexation of Humic Substances with the Stockholm Humic Model. In: *Journal of colloid and interface science* 244 (1), S. 102–112. DOI: 10.1006/jcis.2001.7871.

Gutiérrez-Ruiz, M. E.; Ceniceros-Gómez, A. E.; Villalobos, M.; Romero, F.; Santiago, P. (2012): Natural arsenic attenuation via metal arsenate precipitation in soils contaminated with metallurgical wastes. II. Cumulative evidence and identification of minor processes. In: *Applied Geochemistry* 27 (11), S. 2204–2214. DOI: 10.1016/j.apgeochem.2012.02.021.

Jang, Y-C; Townsend, T. G.; Ward, M.; Bitton, G. (2002): Leaching of arsenic, chromium, and copper in a contaminated soil at a wood preserving site. In: *Bulletin of environmental contamination and toxicology* 69 (6), S. 808–816. DOI: 10.1007/s00128-002-0132-4.

Jernlås, Rikard; Karlgren, Bengt (2009): Asbro Gamla Impregnering. Huvudstudie. VATTENFALL Power Consultant AB.

Jiang, Wei; Zhang, Shuzhen; Shan, Xiao-Quan; Feng, Muhua; Zhu, Yong-Guan; McLaren, Ron G. (2005): Adsorption of arsenate on soils. Part 2: modeling the relationship between adsorption capacity and soil physiochemical properties using 16 Chinese soils. In: *Environmental pollution (Barking, Essex : 1987)* 138 (2), S. 285–289. DOI: 10.1016/j.envpol.2005.03.008.

Liu, Hui-Li; Zhu, Yi-Nian; Yu, Hong-Xia (2009): Solubility and stability of lead arsenates at 25 degrees C. In: *Journal of environmental science and health. Part A, Toxic/hazardous substances & environmental engineering* 44 (13), S. 1465–1475. DOI: 10.1080/10934520903217856.

Lumsdon, D.G; Meeussen, J.C.L; Paterson, E.; Garden, L.M; Anderson, P. (2001): Use of solid phase characterisation and chemical modelling for assessing the behaviour of arsenic in contaminated soils. In: *Applied Geochemistry* 16 (6), S. 571–581. DOI: 10.1016/S0883-2927(00)00063-9.

Magalhaes, Maria Clara F.; Silva, Maria Celina M. (2003): Stability of Lead(II) Arsenates. In: *Monatshefte für Chemie / Chemical Monthly* 134 (5), S. 735–743. DOI: 10.1007/s00706-002-0581-9.

Manning, Bruce A.; Fendorf, Scott E.; Bostick, Benjamin; Suarez, Donald L. (2002): Arsenic(III) Oxidation and Arsenic(V) Adsorption Reactions on Synthetic Birnessite. In: *Environ. Sci. Technol.* 36 (5), S. 976–981. DOI: 10.1021/es0110170.

Manning, Bruce A.; Goldberg, Sabine (1997): Adsorption and Stability of Arsenic(III) at the Clay Mineral−Water Interface. In: *Environ. Sci. Technol.* 31 (7), S. 2005–2011. DOI: 10.1021/es9608104.

Martinez-Villegas, Nadia; Briones-Gallardo, Roberto; Ramos-Leal, Jose A.; Avalos-Borja, Miguel; Castanon-Sandoval, Alan D.; Razo-Flores, Elias; Villalobos, Mario (2013): Arsenic mobility controlled by solid calcium arsenates: a case study in Mexico showcasing a potentially widespread environmental problem. In: *Environmental pollution (Barking, Essex : 1987)* 176, S. 114–122. DOI: 10.1016/j.envpol.2012.12.025.

Moldovan, Brett J.; Hendry, M. Jim (2005): Characterizing and Quantifying Controls on Arsenic Solubility over a pH Range of 1−11 in a Uranium Mill-Scale Experiment. In: *Environ. Sci. Technol.* 39 (13), S. 4913–4920. DOI: 10.1021/es0482785.

Moore, Johnnie N. (1990): Reaction Scheme for the Oxidation of As(III) to As(V) by Birnessite. In: *Clays and Clay Minerals* 38 (5), S. 549–555. DOI: 10.1346/CCMN.1990.0380512.

Pantsar-Kallio, Mari; Manninen, Pentti K.G. (1997): Speciation of mobile arsenic in soil samples as a function of pH. In: *Science of The Total Environment* 204 (2), S. 193–200. DOI: 10.1016/S0048-9697(97)00176-9.

Sadiq, Muhammad (1995): Arsenic chemistry in soils: An overview of thermodynamic predictions and field observations. In: *Water Air Soil Pollut* 93 (1-4), S. 117–136. DOI: 10.1007/BF02404751.

Smith, E.; Naidu, R.; Alston, A. M. (2002): Chemistry of Inorganic Arsenic in Soils. In: *Journal of Environmental Quality* 31 (2), S. 557–563. DOI: 10.2134/jeq2002.5570.

Tiberg, Charlotta; Kumpiene, Jurate; Gustafsson, Jon Petter; Marsz, Aleksandra; Persson, Ingmar; Mench, Michel; Kleja, Dan B. (2016): Immobilization of Cu and As in two contaminated soils with zero-valent iron – Long-term performance and mechanisms. In: *Applied Geochemistry* 67, S. 144–152. DOI: 10.1016/j.apgeochem.2016.02.009.

Tournassat, Christophe; Charlet, Laurent; Bosbach, Dirk; Manceau, Alain (2002): Arsenic(III) Oxidation by Birnessite and Precipitation of Manganese(II) Arsenate. In: *Environ. Sci. Technol.* 36 (3), S. 493–500. DOI: 10.1021/es0109500.

Villalobos, M.; García-Payne, D. G.; López-Zepeda, J. L.; Ceniceros-Gómez, A. E.; Gutiérrez-Ruiz, M. E. (2010): Natural Arsenic Attenuation via Metal Arsenate Precipitation in Soils Contaminated with Metallurgical Wastes. I. Wet Chemical and Thermodynamic Evidences. In: *Aquat Geochem* 16 (2), S. 225–250. DOI: 10.1007/s10498-009-9065-4.

Violante, Antonio; Pigna, Massimo (2002): Competitive Sorption of Arsenate and Phosphate on Different Clay Minerals and Soils. In: *Soil Science Society of America Journal* 66 (6), S. 1788. DOI: 10.2136/sssaj2002.1788.

Williams, L. Elizabeth; Barnett, Mark O.; Kramer, Timothy A.; Melville, Joel G. (2003): Adsorption and Transport of Arsenic(V) in Experimental Subsurface Systems. In: *Journal of Environment Quality* 32 (3), S. 841. DOI: 10.2134/jeq2003.8410.

Xu, H.; Allard, B.; Grimvall, A. (1988): Influence of pH and organic substance on the adsorption of As(V) on geologic materials. In: *Water Air Soil Pollut* 40 (3-4), S. 293–305. DOI: 10.1007/BF00163734.

8 Appendix

Table 1 Recipe for the Pukeberg top and bottom layers: final concentration of HNO3 added to the soil solution to receive a desired pH value.

pH	0-14 cm	14-28 cm
	concentration	
8.18	0	0
7	3.4 mM HNO_3	2.8 mM HNO_3
6	7.3 mM HNO_3	6 mM HNO_3
5	12 mM HNO_3	7.6 mM HNO_3
4	17.5 mM HNO_3	10 mM HNO_3
3	24.6 mM HNO_3	17.5 mM HNO_3

Table 2 Recipe for the Åsbro top and bottom layers: final concentration of HNO3 added to the soil solution to receive a desired pH value.

4-17 cm		Åsbro 17-30 cm	
pH	**concentration**	**pH**	**concentration**
6.7	1.2 mM NaOH	**7.3**	1 mM NaOH
6	0	**6.6**	0
5.1	2.5 mM HNO_3	**5.6**	2.5 mM HNO_3
4.6	7.2 mM HNO_3	**4.9**	6.4 mM HNO_3
4	10 mM HNO_3	**4.1**	10 mM HNO_3
3	21 mM HNO_3	**2.9**	19 mM HNO_3
2.4	30 mM HNO_3	**2.3**	28 mM HNO_3

Table 3 Kinetic table for the Pukeberg top and bottom layers measured for samples to which 17 mmol/L HNO_3 (top layers) and 10 mmol/L HNO3 (bottom layers) had been added

layers	Days	pH	As ug/L
0-14cm	1	3.2515	716
	1	3.2515	560
	5	3.6685	177
	5	3.6685	229
	30	4.469	32.1
	30	4.469	30
14-28cm	1	3.824	220
	1	3.824	215
	5	4.2065	61.4
	5	4.2065	61.7
	30	4.827	3.63
	30	4.827	9.24

Table 4 Kinetic table for the Åsbro top and bottom layers measured for samples to which 28-30 mmol/L HNO_3 had been added.

layers	days	pH	As mg/L
4-17cm	1	2.27	57.9
	1	2.27	56.2
	5	2.46	38.9
	5	2.46	43.5
	33	2.68	31.44
	33	2.68	31.28
	61	2.86	19
	61	2.86	27.64
	90	2.98	11.2
	90	2.98	14.6
17-30cm	1	2.2	74.3
	1	2.2	74
	5	2.33	55.4
	5	2.33	58
	33	2.66	36.08
	33	2.66	34.88
	61	2.78	22.92
	61	2.78	25.32
	90	2.89	15
	90	2.89	17.48

Table 5 Kinetic table for the Pukeberg top and bottom layers measured for samples to which no acid or base had been added

layers	days	pH	As ug/L
0-14cm	1	8.18	71.7
	1		69.5
	5	8.13	78.5
	5		89.6
	30	7.70	83.6
	30		77.2
14-28cm	1	8.15	50.8
	1		51.9
	5	8.21	63.8
	5		61.5
	30	7.80	52
	30		55.5

Table 6 Kinetic table of the Åsbro top and bottom layers measured for samples to which no acid or base had been added

layers	days	pH	As mg/L
4-17cm	1	6.09	0.99
	1	6.09	1.02
	5	6.07	1.65
	5	6.07	1.47
	33	6.07	2.05
	33	6.07	1.76
	61	6.27	1.75
	61	6.27	1.94
	90	6.35	2.26
	90	6.35	2.07
17-30cm	1	6.65	1.37
	1	6.65	1.41
	5	6.74	2.03
	5	6.74	1.99
	33	6.65	2.54
	33	6.65	2.68
	61	6.67	2.84
	61	6.67	2.93
	90	7	3.00
	90	7	3.09

Table 7 CEC table of the Åsbro and Pukeberg top and bottom layers

Element	Åsbro 4-17 cm (cmol(+)/kg)	Åsbro 17-29 cm (cmol(+)/kg)	Pukeberg 0-14 cm (cmol(+)/kg)	Pukeberg 14-28 cm (cmol(+)/kg)
Acidity	2.796	1.369	<0.2	<0.2
Mn	0.020	0.030	0.005	0.005
Mg	0.576	0.558	0.081	0.080
Ca	4.731	7.323	10.658	7.967
Na	0.021	0.015	0.055	0.030
K	0.108	0.089	0.107	0.106
CEC	8.252	9.384	10.906	8.187

Table 8 Geochemical active fraction for the Åsbro and Pukeberg top and bottom layers

Element	Åsbro 4-17cm mmol/L	Åsbro 17-30cm mmol/L	Pukeberg 0-14cm mmol/L	Pukeberg 14-28cm mmol/L
Ca	5.245	4.928	8.039	7.042
Fe	0.984	1.051	0.711	0.632
K	0.269	0.186	0.149	0.164
Mg	1.795	0.671	0.242	0.218
Na	0.160	0.093	0.151	0.145
Si	3.267	1.143	1.673	1.562
Al	2.624	2.151	4.875	4.967
As	1.335	1.453	0.030	0.023
Ba	0.042	0.046	0.152	0.124
Cd	0.001	0.000	0.004	0.004
Co	0.001	0.001	0.001	0.001
Cr	0.368	0.453	0.002	0.001
Cu	0.131	0.328	0.016	0.008
Mn	0.923	0.575	0.189	0.148
Mo	0.000	0.000	0.000	0.000
Ni	0.002	0.003	0.001	0.001
P	0.784	1.018	0.568	0.578
Pb	0.193	0.117	0.153	0.124
Sr	0.009	0.012	0.012	0.011
Zn	2.107	1.525	0.360	0.231
V	0.008	0.009	0.004	0.003

Table 9 Oxalate extraction for the Åsbro and Pukeberg top and bottom layers

Element	Åsbro 4-17cm mmol/L	Åsbro 17-30cm mmol/L	Pukeberg 0-14cm mmol/L	Pukeberg 14-28cm mmol/L
Ca	0.094	0.089	0.119	0.122
Fe	2.699	2.988	1.881	1.376
K	0.137	0.105	0.112	0.088
Mg	0.588	0.394	0.136	0.082
Na	0.107	0.116	0.126	0.053
Si	1.001	0.555	1.229	1.005
Al	1.744	1.577	3.517	3.178
As	1.337	1.607	0.037	0.022
Ba	0.020	0.023	0.074	0.051
Cd	0.000	0.000	0.001	0.001
Co	0.001	0.001	0.001	0.001
Cr	0.318	0.420	0.002	0.001
Cu	0.125	0.333	0.009	0.006
Mn	0.716	0.618	0.154	0.105
Mo	0.001	0.000	0.000	0.000
Ni	0.002	0.003	0.001	0.001
P	0.488	0.570	0.444	0.360
Pb	0.033	0.023	0.025	0.019
Sr	0.001	0.001	0.001	0.001
Zn	1.512	1.208	0.196	0.116
V	0.008	0.010	0.004	0.003

Table 10 Batch experiment results for the Pukeberg top layers

Sample	exp pH	pH	DOC	PO4	As	Pb	P	Ca	Fe	K	Mg	Na	Si	Al	Ba	Cd	Cr	Cu	Mn	Zn
			mg/l	mg/l	ug/l	µg/l	µg/l	mg/l	mg/l	mg/l	mg/l	mg/l	mg/l	ug/l	ug/l	µg/l	µg/l	µg/l	µg/l	µg/l
PB1_1_0.45	3	3.12	8.38	4.43	346	9970	1480	264	2.140	5.75	3.93	249	32.7	65200	15700	320	20.6	180	8030	16100
PB1_2_0.45	3	3.06	9.08	4.7	354	9430	1640	259	2.420	5.8	3.85	250	33.5	67300	15700	387	21.6	174	7940	17600
PB1_1_10kDa	3	3.12	8.84		340	9830	1360	261	2.020	5.6	3.85	244	31.6	63800	15400	316	20.2	179	7910	15900
PB1_2_10kDa	3	3.06	9.13		342	9310	1560	252	2.320	5.6	3.7	247	32.1	65800	15300	390	22.5	174	7750	17200
PB1_1_0.45	4	3.75	4.1	1.4	163	4870	415	280	0.335	5.68	3.6	235	25.6	35600	15700	436	3.59	57	6620	79.3
PB1_2_0.45	4	3.58	5.14	1.98	209	4920	648	264	0.588	5.3	3.7	246	27.9	40500	15000	341	5.26	85.9	6750	69
PB1_1_10kDa	4	3.75	4.47		177	4760	386	275	0.320	5.56	3.57	229	24.9	35200	15500	430	3.41	55.2	6480	78
PB1_2_10kDa	4	3.58	5.54		229	4880	718	260	0.550	5.27	3.6	229	26.4	40000	14700	341	5.4	80.5	6790	69.9
PB1_1_0.45	5	4.88	2.35	0.113	64.4	365	77.2	214	0.038	4.22	2.57	242	17.3	9720	9720	184	0.783	6.16	3980	13500
PB1_2_0.45	5	4.72	1.73	0.167	57.2	479	81.5	207	0.043	4.18	2.59	245	17.6	12200	10100	198	0.661	6.65	4050	13500
PB1_1_10kDa	5	4.88	1.75		61.8	346	69.2	211	0.030	4.14	2.52	238	16.9	9560	9520	182	0.875	6.58	3890	13300
PB1_2_10kDa	5	4.72	1.84		63.7	472	65.2	205	0.038	4.21	2.58	243	17.4	12100	10000	197	0.701	7.48	3990	13400
PB1_1_0.45	6	6.11	1.27	0.056	25.7	33.7	24.3	156	0.013	3.39	1.47	257	9.98	589	5060	52.9	0.189	2.02	1260	3410
PB1_2_0.45	6	6.13	1.38	0.04	26.5	29.6	27.4	155	0.013	3.12	1.48	260	10.1	557	4960	51.9	0.185	2.1	1260	3200
PB1_1_10kDa	6	6.11	1.41		21.4	32.3	25.4	151	0.008	3.46	1.41	250	9.58	636	4880	51.6	0.175	1.94	1220	3340
PB1_2_10kDa	6	6.13	1.45		25	29.5	28.5	148	0.009	2.97	1.42	247	9.59	601	4730	48.4	0.196	1.85	1190	3100
PB1_1_0.45	7	6.95	1.19	0.055	24.2	12.6	27.2	108	0.005	2.46	0.90	231	5.65	38.1	2870	15.3	0.139	1.11	147	165
PB1_2_0.45	7	6.98	1.1	0.052	21.4	12.8	22.8	105	0.004	2.47	0.87	229	5.42	30.9	2800	13.1	<0.1	1.09	170	145
PB1_1_10kDa	7	6.95	1.48		22.9	10.7	25.4	106	<0.004	2.47	0.89	232	5.64	33.9	2850	16.1	0.1	1.6	146	152
PB1_2_10kDa	7	6.98	1.44		24.9	11.4	29.5	106	<0.004	2.5	0.87	227	5.42	35	2790	14.2	0.127	1.54	171	148
PB1_1_0.45	8.18	8.11	1.9	0.27	82.3	4.61	62.1	29.3	0.006	1.91	0.22	225	2.22	190	864	0.76	0.535	1.61	0.98	6.57
PB1_2_0.45	8.18	8.14	1.72	0.28	83.1	8.22	61	28.4	0.017	1.89	0.21	215	2.08	192	832	0.741	0.571	1.64	2.18	15.6
PB1_1_10kDa	8.18	8.11	1.64		78.5	3.08	64.5	27.7	0.003	1.88	0.20	210	2.07	178	812	0.8	0.416	1.8	0.46	21.2
PB1_2_10kDa	8.18	8.14	1.62		89.6	3.08	57.7	28.3	0.003	1.89	0.21	216	2.04	178	824	0.718	0.555	1.83	0.45	18.7

Table 11 Batch experiment results for the Pukeberg bottom layers

Sample	exp pH	pH	DOC	PO4	As	Pb	P	Ca	Fe	K	Mg	Na	Si	Al	Ba	Cd	Cr	Cu	Mn	Zn
			mg/l	mg/l	ug/l	µg/l	µg/l	mg/l	mg/l	mg/l	mg/l	mg/l	mg/l	ug/l	ug/l	µg/l	µg/l	µg/l	µg/l	µg/l
PB1_1_0.45	3	2.82	10.3	7.48	284	8130	2510	180	3.46	6.19	3.29	233	30.1	69400	10800	221	25.8	191	5290	59.4
PB1_2_0.45	3	2.82	11	9.88	383	7850	3430	185	2.87	5.74	2.99	238	29.4	69300	10600	237	22.5	183	5150	60.9
PB1_1_10kDa	3	2.82	10.7		271	8100	2560	178	3.37	6.15	3.25	232	29.3	68600	10700	219	23.6	190	5210	50
PB1_2_10kDa	3	2.82	10.8		381	7730	3470	181	2.77	5.65	2.92	234	28.2	68100	10400	232	20.6	179	5060	39
PB1_1_0.45	4	4.14	2.63	0.348	64.5	1400	90.5	154	0.106	4.57	2.25	239	17.1	21800	8400	192	1.42	27.4	3570	72.4
PB1_2_0.45	4	4.28	2.46	0.349	67.8	1220	109	163	0.097	4.51	2.33	239	17	21700	8410	277	1.14	20.3	3540	80.3
PB1_1_10kDa	4	4.14	2.64		61.4	1370	97	156	0.100	4.57	2.24	240	17.2	22000	8460	193	1.6	28.2	3590	68.8
PB1_2_10kDa	4	4.28	2.82		61.7	1210	92.6	162	0.074	4.54	2.31	241	17	21800	8380	279	1.22	20.4	3490	72
PB1_1_0.45	5	5.44	1.12	0.05	26.6	118	36.2	137	0.022	4.26	1.75	240	11.5	5170	5220	97	0.174	3.11	1830	6030
PB1_2_0.45	5	5.09	1.06	0.066	33	162	41.7	132	0.025	3.95	1.74	247	11.7	6640	5600	134	0.52	3.75	1920	5880
PB1_1_10kDa	5	5.44	1.26		31.4	124	38.8	135	0.020	4.22	1.7	237	11.3	5190	5130	96.7	0.288	2.98	1800	5960
PB1_2_10kDa	5	5.09	1.23		30.7	169	40.5	127	0.021	3.79	1.66	231	11.3	6360	5350	125	0.357	3.08	1860	5650
PB1_1_0.45	6	5.62	1.44	<0.040	26	60.3	29.6	123	0.018	3.72	1.55	250	9.85	3010	4450	67.9	0.291	2.36	1390	4140
PB1_2_0.45	6	5.59	1.41	<0.040	23.5	88.6	29	127	0.016	3.92	1.53	255	9.87	2850	4550	144	0.297	2.98	1270	3850
PB1_1_10kDa	6	5.62	1.46		29.9	60.7	33.9	122	0.014	3.82	1.52	245	9.63	3090	4370	66.8	0.325	2.69	1370	4120
PB1_2_10kDa	6	5.59	1.44		25.6	93.2	30	126	0.014	3.77	1.5	252	9.66	3010	4490	142	0.339	2.48	1250	3860
PB1_1_0.45	7	6.95	1.27	0.063	24.5	9.08	35.4	85.1	0.022	2.89	0.86	230	4.86	79.6	2130	14.1	0.0656	2.11	79.1	119
PB1_2_0.45	7	6.83	1.13	0.069	25.1	8.87	28.7	85.8	0.008	2.98	0.85	237	4.98	63.6	2220	13	0.179	1.76	78.6	106
PB1_1_10kDa	7	6.95	1.37		22.6	7.54	27.9	84.9	0.005	2.95	0.87	232	4.89	53.1	2130	13.1	0.104	1.74	80.5	115
PB1_2_10kDa	7	6.83	1.49		24.9	7.43	30.8	84.3	0.004	2.96	0.84	233	4.92	61.1	2190	14	0.176	1.7	77.9	112
PB1_1_0.45	8.18	8.23	1.52	0.253	64.3	3.11	67.3	26.4	0.012	2.29	0.27	219	1.77	261	703	0.515	0.614	1.74	1.18	5.27
PB1_2_0.45	8.18	8.20	1.53	0.227	62	5.51	72.8	27	0.011	2.34	0.27	225	1.82	269	725	0.64	0.623	1.78	2.46	10.2
PB1_1_10kDa	8.18	8.23	1.6		63.8	2.16	65.5	25.9	0.002	2.3	0.26	221	1.73	242	687	0.441	0.446	1.76	0.38	14.2
PB1_2_10kDa	8.18	8.20	1.47		61.5	2.29	60.6	26	0.002	2.28	0.26	216	1.73	246	689	0.469	0.575	1.52	0.357	9.22

Table 12 Batch experiment results for the Åsbro top layers

samples	exp pH	pH	TOC	PO4	Ca	Fe	Mg	Al	As	Ba	Cr	Cu	Mn	Pb	K	Na	Si	P	Zn
			mg/l	mg/l	mg/l	mg/l	mg/l	µg/l	ug/l	µg/l	µg/l	µg/l	µg/l	µg/l	mg/l	mg/l	mg/l	µg/l	µg/l
Ab_1_0.45	2.4	2.412	19.1	75.7	190	1.04	41.6	61500	39300	5440	3420	5900	48100	8280	11.2	230	92.6	6270	139000
Ab_2_0.45	2.4	2.478	20.4	73.6	172	1.51	36.3	61300	43700	5340	4750	6190	48100	6800	10.2	233	79.6	7330	141000
Ab_1_10kDa	2.4	2.412	15.7		189	1	41.8	61700	38900	5490	3350	5880	47800	8200	11.2	234	85.1	6500	139000
Ab_2_10kDa	2.4	2.478	14		172	1.47	36.4	61800	43500	5380	4690	6150	48200	6830	10.3	233	74	7370	141000
Ab_1_0.45	3	3.082	14.6	45.6	164	0.264	33.2	29200	29800	4610	835	3800	35000	1570	9.53	227	69.3	3230	134000
Ab_2_0.45	3	3.115	14.1	41.4	158	0.245	32.8	29200	29500	4620	805	3820	33900	2870	9.65	227	69.6	2910	140000
Ab_1_10kDa	3	3.082	9.4		163	0.262	33.6	29500	30100	4660	814	3830	35200	1520	9.67	231	65.4	2970	134000
Ab_2_10kDa	3	3.115	8.3		159	0.242	32.9	29500	29900	4680	793	3830	34200	2870	9.79	232	65.8	2820	138000
Ab_1_0.45	4	4.187	8.37	23.2	111	0.0469	21.7	3090	17600	2340	134	681	14600	97.1	6.82	222	39	746	92500
Ab_2_0.45	4	4.273	8.17	21.9	110	0.0461	22.1	2880	16500	2340	131	617	13700	135	6.68	222	40.4	700	89700
Ab_1_10kDa	4	4.187	5		111	0.0537	22	3120	17600	2370	139	687	14700	103	6.98	228	39.1	732	93800
Ab_2_10kDa	4	4.273	5		113	0.0441	22.8	2930	16900	2410	129	633	13900	143	7	231	41.2	875	91000
Ab_1_0.45	4.6	4.537	6.12	19.6	83.6	0.0346	13	883	13800	1070	90.1	156	4680	25	5.04	229	21.7	965	4.89
Ab_2_0.45	4.6	4.658	6	19.5	93.8	0.0354	12.6	761	14100	996	82.1	137	4300	20.3	4.85	212	21.7	961	5.39
Ab_1_10kDa	4.6	4.537	5.77		83.3	0.038	12.9	886	14000	1060	94.3	151	4600	20.6	4.9	227	21.2	1060	5.75
Ab_2_10kDa	4.6	4.658	5.74		94.2	0.0345	12.7	772	14200	999	81.6	132	4270	17.2	4.94	215	21.3	1030	4.94
Ab_1_0.45	5.1	5.122	6.87	8.46	37.2	0.0752	4.16	234	7330	437	65.4	67.9	848	16.3	2.8	227	4.7	841	19100
Ab_2_0.45	5.1	5.089	6.95	8.24	37.8	0.0844	4.2	223	6620	422	62.8	64	761	12.6	2.89	223	4.78	845	18600
Ab_3_0.45	5.1	5.089	4.92		37.8	0.0474	4.02	219	6160	368	69.4	55.2	582	10.4	2.89	224	4.15	661	3.35
Ab_1_10kDa	5.1	5.122	5		37.3	0.037	4.12	210	7230	429	60.9	62.6	841	11.6	2.78	224	4.67	804	19100
Ab_2_10kDa	5.1	5.089	5.4		38.1	0.0366	4.21	196	6680	420	55.7	60.7	757	6.48	2.9	224	4.78	835	18600
Ab_3_10kDa	5.1	5.089	4.72		37.8	0.0334	4.01	210	6190	366	70.3	54.1	556	7.62	2.92	224	4.12	687	3.12
Ab_1_0.45	6	5.968	8.35	2.71	10.2	0.618	1.42	332	1830	92.9	111	54.3	194	99.7	2	207	2.33	216	2450
Ab_2_0.45	6	6.059	7.07	2.58	10.3	0.869	1.41	330	1770	91.2	106	53.9	174	90.7	2.04	207	2.42	193	2450
Ab_3_0.45	6	6.059	5.24		11.5	0.185	1.46	154	1870	93.9	64.6	44.1	74.9	28.4	2.36	221	2.14	203	3.96

Ab_1_10kDa	6	5.968	5.1		10.8	0.0413	1.5	88.1	1650	88.5	40.6	33.3	33	4.18	2.14	220	2.15	153	2360
Ab_2_10kDa	6	6.059	5.4		9.92	0.0379	1.39	85.2	1470	81.7	35.4	30.9	31.4	4.67	2.01	206	1.98	144	2160
Ab_3_10kDa	6	6.059	4.65		11	0.0362	1.43	76.2	1720	79.1	46.5	33.2	17.3	2.7	2.24	220	1.9	161	3.58
Ab_1_0.45	7	7.05	11.2	3.83	5.14	1.7	0.724	844	2520	60.9	261	119	367	250	2.09	244	3.52	350	10.6
Ab_2_0.45	7	6.92	10.2	3.34	4.97	1.18	0.695	559	2170	47.1	185	96.8	247	187	2.11	248	3.38	262	8.93
Ab_1_10kDa	7	7.05	7.07		4.35	0.0441	0.628	65.4	1640	27.4	50.4	43.3	3.95	3.46	1.98	244	2.15	172	6.39
Ab_2_10kDa	7	6.92	7.18		4.39	0.0533	0.634	66.8	1600	28.3	51.2	43.3	5.66	5.91	1.98	243	2.17	154	5.85

Table 13 Batch experiment results for the Åsbro bottom layers

samples	exp pH	pH	TOC	PO4	Ca	Fe	Mg	Al	As	Ba	Cr	Cu	Mn	Pb	K	Na	Si	P	Zn
			mg/l	mg/l	mg/l	mg/l	mg/l	µg/l	ug/l	µg/l	µg/l	µg/l	µg/l	µg/l	mg/l	mg/l	mg/l	µg/l	µg/l
Ab_1_0.45	2.3	2.378	20	101	188	2.36	20.2	53300	54500	5840	6790	17400	34800	5300	6.75	231	37.8	11100	104000
Ab_2_0.45	2.3	2.397	18.8	99.6	187	2.37	17.1	54800	57200	6340	7080	18200	35800	6030	6.75	232	33.4	11100	111000
Ab_1_10kDa	2.3	2.378	15.3		192	2.38	20.5	54200	55400	5870	6940	17400	35300	5350	6.73	230	38.3	11100	107000
Ab_2_10kDa	2.3	2.397	16.8		189	2.4	17.3	55800	58000	6390	7190	18500	36100	5980	6.89	234	34	11100	113000
Ab_1_0.45	2.9	2.939	15.5	71.9	172	0.424	15.2	30300	45200	5270	1590	12700	28900	1410	6.17	236	26.1	6990	103000
Ab_2_0.45	2.9	2.97	14.9	71.2	176	0.414	14.3	30400	45200	5370	1590	12500	28200	1380	6.38	228	26.1	6520	104000
Ab_1_10kDa	2.9	2.939	13.3		175	0.433	15.6	31200	46400	5410	1620	12900	29800	1440	6.52	241	27	7040	106000
Ab_2_10kDa	2.9	2.97	13.2		173	0.405	14	29600	44200	5230	1560	12300	28400	1500	6.32	225	25.7	6750	103000
Ab_1_0.45	4.1	4.117	9.34	47.2	131	0.06	10.3	5520	30900	2100	223	1750	10400	48.5	4.44	228	14.1	3440	62100
Ab_2_0.45	4.1	4.175	9.21	46.1	129	0.0613	10.3	5280	30200	2120	219	1740	11000	49.9	4.5	225	14.2	3450	61000
Ab_3_0.45	4.1	4.117	7.25		140	0.0509	9.78	5970	34300	2050	237	1720	8980	49.4	4.73	227	13.9	3470	8.3
Ab_1_10kDa	4.1	4.117	8		127	0.0612	10	5340	30300	2050	213	1700	10200	47.5	4.34	223	13.9	3320	61200
Ab_2_10kDa	4.1	4.175	8.1		131	0.0621	10.3	5310	30700	2110	220	1730	11100	47.7	4.29	224	14.4	3350	62200
Ab_3_10kDa	4.1	4.117	7.21		141	0.0536	9.83	5960	34100	2040	237	1700	8940	54.9	4.76	223	13.6	3540	8.77
Ab_1_0.45	4.9	4.77	5.99	35.4	102	0.0359	6.78	1650	22800	931	121	440	3130	12.3	3.79	232	8.53	3200	8.06
Ab_2_0.45	4.9	4.69	5.97	35.4	102	0.0343	6.61	1580	22600	916	112	424	2930	18.3	3.64	216	8.05	3130	8.33

Ab_1_10kDa	4.9	4.77	6.13		101	0.0358	6.74	1640	22500	929	120	438	3090	10.8	3.7	230	8.4	3080	7.38
Ab_2_10kDa	4.9	4.69	6.1		99.8	0.0345	6.49	1540	22000	907	107	410	2850	14.9	3.49	213	7.88	3210	8.54
Ab_1_0.45	5.6	5.498	5.57	12	46.9	0.0439	3.47	191	9840	290	75.1	118	237	4.57	2.55	221	3.54	1540	6410
Ab_2_0.45	5.6	5.521	5.7	12.1	47.4	0.0615	3.48	191	9770	290	78.1	123	238	6.57	2.62	221	3.71	1500	6220
Ab_1_10kDa	5.6	5.498	5		47.5	0.0215	3.52	176	9880	293	71.7	112	240	2.22	2.58	225	3.62	1520	6460
Ab_2_10kDa	5.6	5.521	5		47	0.0216	3.49	173	9780	290	69.9	115	230	2.45	2.65	226	3.66	1550	6120
Ab_1_0.45	6.7	6.668	4.8	2.84	12.2	0.327	1.09	125	2130	62.8	131	76.1	33.6	27.7	1.99	209	1.61	106	548
Ab_2_0.45	6.7	6.565	5.7	2.87	11.7	0.556	1.04	147	2230	63.7	140	83.9	54.1	39	1.87	208	1.57	124	572
Ab_3_0.45	6.7	6.668	3.77		13	0.317	1.07	114	2500	60.1	153	95.8	31.5	29.5	2.14	224	1.63	130	9.56
Ab_1_10kDa	6.7	6.668	5		12.1	0.0108	1.08	24.5	2030	58	92.8	51	7.23	1.01	2.21	212	1.51	88.4	459
Ab_2_10kDa	6.7	6.565	5		11.2	0.0119	1.01	38.7	1990	57	84.9	51	10.9	2.48	1.82	204	1.4	97.1	491
Ab_3_10kDa	6.7	6.668	3.58		12.9	0.0163	1.06	33.1	2380	56.1	116	67.9	3.4	1.48	2.11	223	1.52	97.8	8.44
Ab_1_0.45	7.3	7.476	6.96	4.68	6.13	0.847	0.476	261	3590	37.2	187	134	73.7	67	1.82	235	1.79	213	14.2
Ab_2_0.45	7.3	7.352	7.52	5.14	5.95	0.491	0.478	188	3650	31.1	157	131	42	43.3	1.97	246	1.83	194	14.1
Ab_1_10kDa	7.3	7.476	4.82		5.64	0.0173	0.453	36.4	3200	25	82.1	64.6	4.49	1.5	1.78	235	1.53	149	11.4
Ab_2_10kDa	7.3	7.352	4.61		5.69	0.0201	0.458	39.9	3480	21	80.3	73.7	5.7	1.9	1.94	245	1.61	156	11.4